39th Plasmadynamics and Lasers Conference<BR>
23 - 26 June 2008, Seattle, Washington

AIAA 2008-3788

# A Critical Review of Electric and Electromagnetic Flow Control Research Applied to Aerodynamics

Eric M. Braun,* Frank K. Lu,† and Donald R. Wilson,‡
*University of Texas at Arlington, Arlington, Texas, 76019, USA*

**Fifty years ago, publications began to discuss the possibilities of electromagnetic flow control (EMFC) to improve aerodynamic performance. This led to an era of research that focused on coupling the fundamentals of magnetohydrodynamics (MHD) with propulsion, control, and power generation systems. Unfortunately, very few designs made it past an experimental phase as, among other issues, power consumption was unreasonably high. Recent proposed advancements in technology like the MARIAH hypersonic wind tunnel and the AJAX scramjet engine have led to a new phase of MHD research in the aerospace industry, with many interdisciplinary applications. Aside from propulsion systems and channel flow accelerators, electromagnetic flow control concepts applied to control surface aerodynamics have not seen the same level of advancement that may eventually produce a device that can be integrated with an aircraft or missile. Therefore, the purpose of this paper is to review the overall feasibility of the different electric and electromagnetic flow control concepts. Emphasis is placed on EMFC and experimental work.**

## Nomenclature

| | | |
|---|---|---|
| $b$ | = | induced magnetic field, T |
| $B$ | = | magnetic field, T |
| $c_f$ | = | skin friction coefficient |
| *DBD* | = | dielectric barrier discharge |
| $E$ | = | electric field, V/m |
| $e$ | = | electron charge, $-1.602\times10^{-19}$ C |
| *EFC* | = | electrohydrodynamic flow control |
| *EHD* | = | electrohydrodynamics |
| *EMFC* | = | electromagnetic flow control |
| $F$ | = | force, N |
| $F_L$ | = | Lorentz force, N (single particle), N/m$^3$ (ionized particles per unit volume) |
| $I$ | = | current, A |
| $I_{BL}$ | = | $\left(\sigma B^2 L / \left[\rho u_\infty \sqrt{c_f/2}\right]\right)$ boundary layer magnetic interaction parameter |
| $I_{EM}$ | = | $\left(BE\sigma L / \rho u_{BL}^2\right)$ electromagnetic interaction parameter |
| $I_M$ | = | $\left(\sigma B^2 L / \rho u\right)$ magnetic interaction parameter |
| $J$ | = | current field, A/m$^2$ |
| $L$ | = | characteristic length, m |
| *MHD* | = | magnetohydrodynamics |
| $n$ | = | number density, 1/m$^3$ |
| $p$ | = | static pressure, Pa |

* Graduate Research Associate, Aerodynamics Research Center, Department of Mechanical and Aerospace Engineering, Box 19018, Student Member AIAA.
† Professor and Director, Aerodynamics Research Center, Department of Mechanical and Aerospace Engineering, Box 19018, Associate Fellow AIAA.
‡ Professor and Interim Chair, Department of Mechanical and Aerospace Engineering, Box 19018, Associate Fellow AIAA.

$q$ = electric charge, C
$Re_M$ = ( $\mu_0 \sigma u L$ ) magnetic Reynolds number
$r$ = distance, m
$S$ = cross sectional area, $m^2$
$u$ = flow speed, m/s
$WIG$ = weakly ionized gas
$x$ = Cartesian coordinate along streamwise width
$y$ = Cartesian coordinate along spanwise length
$z$ = Cartesian coordinate along transverse height
$Z$ = number of net charges on a particle
$Z_{EHD}$ = ( $\varepsilon_0 E^2 / 2\rho u^2$ ) electrohydrodynamic interaction parameter
$\varepsilon_0$ = permittivity of vacuum constant, $8.854 \times 10^{-12}$ F/m
$\mu_0$ = permeability of vacuum constant, $1.257 \times 10^{-6}$ $N/A^2$
$\rho$ = density, $kg/m^3$
$\rho_e$ = charge density, $C/m^3$
$\sigma$ = conductivity, mho/m

Subscripts
$BL$ = boundary layer
$p$ = particle
$\infty$ = free stream

## I. Introduction

FIFTY years ago, an article appeared describing the prospects for "Magneto-Aerodynamics".[1] In it, Resler and Sears stated that an electromagnetic field could be coupled with an ionized gas flow to accelerate or decelerate it, delay boundary layer separation, or to control skin friction and heat transfer. With several additions since that time, these goals remain the same. The authors also discussed several advancements critical to the progress of electromagnetic flow control. Among them was the ability to solve the complex magnetohydrodynamic equations, which has eased tremendously stemming from the development of more powerful computing hardware and numerical methodologies. Next, Resler and Sears mentioned that more powerful magnets would be needed for ionized fluid flow control. This objective has been achieved to some extent. Electromagnets can produce fields of several tesla, and superconducting magnets can reach tens of tesla. However, the size of these magnets makes integration into an aerospace vehicle problematic. Also, the magnets are dependent upon large power supplies. Research into rare-earth materials has progressed considerably since 1958, with inexpensive neodymium magnets currently available with maximum surface fields in the 0.5–1.0 T range. However, their use for aerodynamic control is limited since their magnetic fields are reduced as temperature is increased, making their incorporation into applications like scramjet inlets difficult if not impractical.

In addition to the strength of the magnetic field, EMFC is also dependent upon the conductivity of the ionized airflow. Resler and Sears believed that artificial seeding of the airflow to create higher plasma conductivities would need development. At the time, plasma jet sources were fully capable of creating high values of conductivity for ground testing. As an example, consider a linear Lorentz force accelerator developed in the 1960's.[2] The accelerator has a square cross-section of 2.54 cm sides and a length of 76 cm. The 60 electrode pairs in the accelerator were powered by a warehouse of 1700 12-V automotive batteries. The accelerator electromagnets were powered with a current of up to 900 A at 80 V. Finally, the plasma generator operated off a 10 MW power supply, and could create a flow with a conductivity of up to 500 mho/m (with seeding). However, the vehicle-scaled power requirement of an air-breathing plasma jet currently may only be met by something like an on-board nuclear reactor. In order to reduce that power requirement, seeding the plasma jet with low ionization energy potassium and cesium compounds was explored, which resulted in a tremendous increase in conductivity relative to the unseeded gas. For instance, a hypersonic vehicle flying at an altitude of 30 km at Mach 16 would ionize the air after a bow shock to $\sigma \approx 0.05$ mho/m. Adding 0.1% potassium by weight could boost the conductivity to roughly 1 mho/m,[3,4] a 20-fold increase.

For control surface aerodynamics, thermal ionization, whether augmented by seeding or not, may not be feasible or even desirable. Seeding also is not desirable for concepts like the MARIAH hypersonic wind tunnel facility[5] or the AJAX scramjet power generator.[6-8] At speeds below that which result in significant shock-induced ionization, EMFC may have serious limitations compared to its overall benefits. A few situations do exist in which ionization is

currently experienced by an aerospace vehicle. For instance, the Space Shuttle interacts with ionized particles while in low Earth orbit[9] and during re-entry, where the re-entry environment has resulted in numerous studies (e.g., Refs. 10 and 11) of how to improve current vehicle designs with the addition of electromagnetic fields. However, with the Space Shuttle's impending retirement and no new prospects for the incorporation of actuators into full-scale space vehicles (assuming the Orion design is nearly finalized), hypersonic missiles may currently be the best near-term candidate for EMFC systems. With that in mind, the flight Mach number may be limited to below about 15, for which artificial creation of an adequate amount of flow conductivity is necessary. Recently, generating a conductive gas, also known as a weakly ionized gas, can be accomplished using high voltage fields, laser beams, or perhaps directed microwaves.[12,13] However, these ionization methods produce a far lower level of conductivity when compared with results from fifty years ago. Experimentally, the maximum realized values of $\sigma$ in air are currently in the 0.1–1.0 mho/m range with high voltage fields. Raising the gas conductivity and minimizing power consumption is obviously a priority if practical aerospace systems are to be realized.

Also of significant note has been the development of flow control systems utilizing only plasma or an electric field. The design of an EFC device with only a high voltage field is much less complex since the field will ionize the air itself. Electrohydrodynamic flow control techniques can be divided into two categories: glow discharge and dielectric barrier discharge. The physics for the two categories is similar. An air gap exists between the anode and cathode region of a glow discharge, while a much thinner dielectric gap is used for DBD systems. Paschen's law states that the electrical breakdown voltage is based on gap distance and pressure. Because the anode and cathode of a DBD are separated by a thin dielectric gap, the electric field strength is increased, which significantly raises the output Coulomb body force. Hence, most glow discharge research has occurred with low pressures while the environment for DBD systems has been closer to atmospheric. Although both systems solve the conductivity generation problem by ionizing the air without a separate system, the value of $\sigma$ is very low (perhaps $10^{-5}$–$10^{-7}$ mho/m). Conveniently, both systems also operate often using less than 1 kW of power.

One may assume the magnitude of the force generated by electric or electromagnetic fields is naturally a reflection of the amount of power consumed. Considering the potential use of each in the aerospace industry, there is a tendency to associate electromagnetic fields with systems consuming a large amount of power. Systems based solely on the Coulomb force have been proposed and used for applications with relatively less power (e.g., electrostatic ion thrusters and ion lifters). Therefore, a very fundamental issue to address for the future of flow control using these fields is defining how much power is needed for an appreciable control force. Put another way, while an electromagnetic field is generally associated with more powerful aerospace applications, an electric field may be all that is necessary to generate a satisfactory control force. The answer to this question will likely cause one to eventually be far more appropriate for use over the other.

Unfortunately, recent experimental results do not address this issue well. Aerospace research involving electromagnetic fields has focused on hypersonic flows,[14] particularly for the augmentation of scramjet propulsion systems. Most work involving MHD and scramjets has been computational, which is clearly understandable due to the cost and complexity of testing. However, this situation has led to significant differences between experimental and computational work. Experimental values of pressure, conductivity and magnetic field strength are usually below what is assumed analytically or in computational simulations. For example, Bruno et al. assumed a magnetic field between 7–17 T as part of a first-order electromagnetic hypersonic propulsion system.[15] In another design, Park et al. computed values of $B$ = 11.28 T, $\sigma$ = 35.87 mho/m (with seeding) and $p$ = 1.25 MPa at the entrance to the scramjet's MHD accelerator.[16] Recent experiments have been generally limited to 0.5–4.0 T, at most a few mho/m, and pressures low enough to have to be stated in torr. Low pressure testing has been a method to increase the magnetic interaction parameter $I_M$ understandably as such conditions facilitate ionization. Little discussion has been articulated on the subject matter of selecting appropriate values of these parameters for aerodynamic control surfaces. Practical values of crucial scaling parameters must be established so as to define what value ranges should be associated with larger, propulsion-associated systems and smaller control surface systems.

On the other hand, electrohydrodynamic flow control (especially with DBDs) has mostly been experimentally demonstrated with low speeds and Reynolds numbers[17] or for bluff bodies. Some high-speed experimentation has appeared in the literature, but the control is more often caused by Joule heating from an electrical arc rather than from the presence of an electrohydrodynamic force. The Reynolds number must be significantly increased for vehicle control surfaces to apply such systems. Based on all of the research in these areas, it is reasonable to observe that EMFC is more appropriate than EFC for hypersonic propulsion systems since it can effectively accommodate larger amounts of energy. However, EFC may be more appropriate for low Reynolds number control systems, and its implementation is relatively simple without the ionization problem. In general, many more possibilities exist for the implementation of EFC and EMFC in systems at conditions other than those presented above.

## II. Electrohydrodynamic versus Magnetohydrodynamic Interaction

The central difference between electrohydrodynamics (EHD) and magnetohydrodynamics (MHD) is the force produced during the interaction of ionized particles with the electric or electromagnetic fields, respectively. For EHD, it is the Coulomb force while for MHD it is the Lorentz force. These interactions are often summed up in one equation written as

$$F_L = q\left(E + u \times B\right). \tag{1}$$

As research in electric and electromagnetic flow control has begun to focus mainly within the boundary layer where $E$ is high and $u$ is low, there is a tendency to observe Eq. (1) and conclude that the presence of a magnetic field has little effect on the magnitude of the body force from a simple order-of-magnitude comparison of the two terms on the right hand side. This conclusion is incorrect since each part of Eq. (1) actually contains an electric field component. Note that the $u \times B$ product is actually an electric field, usually referred to as the internal induced electric field in channel flow applications. The single $E$ term is referred to as the applied (accelerators) or external (generators) electric field. Interaction of only an electric field with ionized particles will produce a body force, but its relative magnitude with respect to the force produced by an electromagnetic field cannot easily be determined by Eq. (1). A strong current field interacting with ionized particles can create an induced magnetic field, but the body force generated from that situation may be negligible for EMFC as will be shown. The concepts above have been well established in the literature.[18,19] A derivation of the EHD and MHD forces is shown below along with a comparison between the effectiveness of each for an example EMFC control surface.

Coulomb's law states that two charged particles exert a mutual force in a direction parallel to the line connecting each particle. If one of these particles is held stationary, it creates an electric field and exerts a force on the other particle, written as

$$F_2 = eZ_2\left[\frac{eZ_1}{4\pi\varepsilon_0}\frac{r_2 - r_1}{\left|r_2 - r_1\right|^3}\right], \tag{2}$$

where the bracketed terms represent the electric field. Similarly, the magnetic force law states that a force is developed between two current carrying wires which is dependent on distance and, additionally, the orientation of the wires. Over a length of wire $dl$ this force is written as

$$dF\left(r\right) = \frac{\mu_0}{4\pi}\frac{II'}{\left|r - r'\right|^3}dl \times \left[dl' \times \left(r - r'\right)\right], \tag{3}$$

where the prime is used to denote the properties of one wire from another. Invoking the Biot-Savart law leads to an expression for the magnetic field at $r$.

$$B\left(r\right) = \frac{\mu_0}{4\pi}\int_{l'}\frac{I'\left(r'\right)dl' \times \left(r - r'\right)}{\left|r - r'\right|^3} \tag{4}$$

Next, using Ampere's law, Eq. (3) can be simplified to

$$dF\left(r\right) = I\left(r\right)dl\left(r\right) \times B. \tag{5}$$

If $S$ denotes the cross-sectional area of the wire, $n$ denotes the number of particles and the subscript $p$ denotes a particle along the wire, then the force is

$$dF = n_p eZ_p u_p \times B. \tag{6}$$

Furthermore, the force on one particle is

$$F_p = eZ_p u_p \times B. \tag{7}$$

Therefore, the combined electric and magnetic forces on a particle are

$$F_p = eZ_p \left( E + u_p \times B \right). \tag{8}$$

Note Eq. (8) has omitted the Hall effect (which can be significant) and ion slip for this example. Also neglecting polarization and magnetization effects, the body force components on an ionized gas or liquid is

$$F = \rho_e E + J \times B. \tag{9}$$

Next, the order of magnitude of these electric and electromagnetic Lorentz force components can be approximated,[18] allowing for a comparison between the two.

$$\rho_e E \approx \frac{\varepsilon_0 E^2}{L} \tag{10}$$

$$F_L \equiv J \times B \approx \sigma \left( E + uB \right) B \tag{11}$$

As an example, consider a flat plate electromagnetic flow control actuator[20] with five surface electrodes each separated by 1.59 cm of dielectric material as shown in Fig. 1. The figure is a computer rendition of an actuator already constructed and tested. The middle and outer electrodes are grounded, while the potential of the central electrodes is 100 V. The length and width of the electrodes are 1.27 and 0.51 cm, respectively. Permanent, NdFeB magnets 1.27 cm square by 2.54 cm long, are located just under the surface. The total magnetic field $B$ is shown in Fig. 2 (as measured across the surface of the plate). Next, assume this device is placed on a missile as a traditional control surface replacement for a flight speed of 1000 m/s. The conductivity of the air is assumed to be 1 mho/m, produced by a separate ionization system. The boundary layer thickness has been arbitrarily set to 2.54 cm and the velocity profile follows a typical turbulent shape. The boundary layer velocity as a function of height off of the flat plate is denoted as $u_{BL}$, and it reaches 700 m/s at $z$ = 1.27 cm, the maximum height where data are discussed in this section. Magnetic field measurements are also available to $z$ = 1.27 cm.

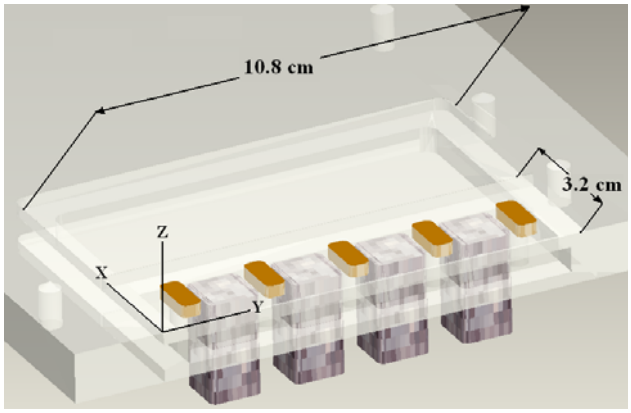


**Figure 1. Image of the five electrode, four magnet actuator plate with dielectric material shown as transparent.**

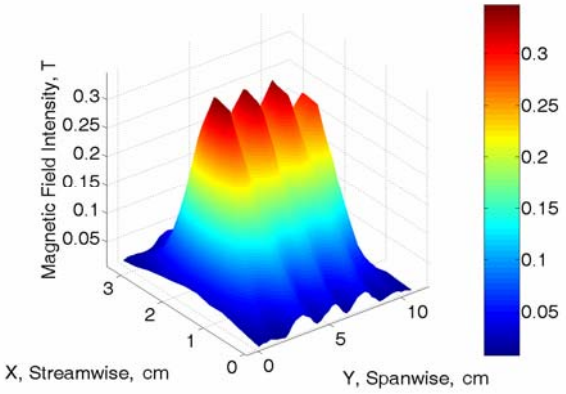


**Figure 2. Total magnetic field located on the surface of the flat plate over the 10.8 × 3.2 cm area.**

Using Eqs. (10) and (11), the ratio of the electrohydrodynamic force to the magnetohydrodynamic force is

$$\frac{F_{EHD}}{F_{MHD}} \equiv \frac{\rho_e E}{J \times B} = \frac{\varepsilon_0 E^2}{L\sigma\left(E + u_\infty B\right)B}. \tag{12}$$

The electric field $E$ has been calculated using a computational MHD code which provides an accurate field with this surface geometry. Finally, a spanwise slice of the electric and magnetic fields has been taken at a streamwise location of 1.8 cm in order to calculate the Lorentz force field. The next set of figures presents the results including a chart showing the local magnetic interaction parameter accounting for the boundary layer flow velocity profile,

$$I_M = \frac{EM\ \ forces}{flow\ inertia} = \frac{\sigma B^2 L}{\rho u_{BL}}, \tag{13}$$

where $L$ is the streamwise length of the electrode/magnet arrangement and the density $\rho$ is approximated as 1 kg/m$^3$ throughout the boundary layer for illustrative purposes (in actuality it will decrease towards the surface). The next six figures should be symmetric, but the measured data points for $B$ and large gradients in $E$ creates dissimilarity.

In Fig. 3, one can see that the magnitude of the Lorentz force produced in part with the NdFeB magnets drops

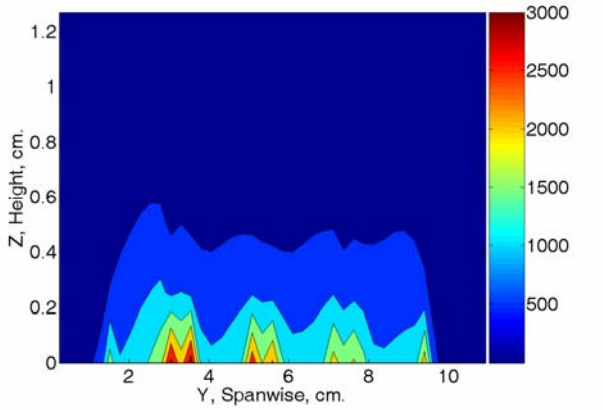


**Figure 3. The Lorentz force (N/m$^2$) across a streamwise slice of the flat plate at $x$ = 1.8 cm.**

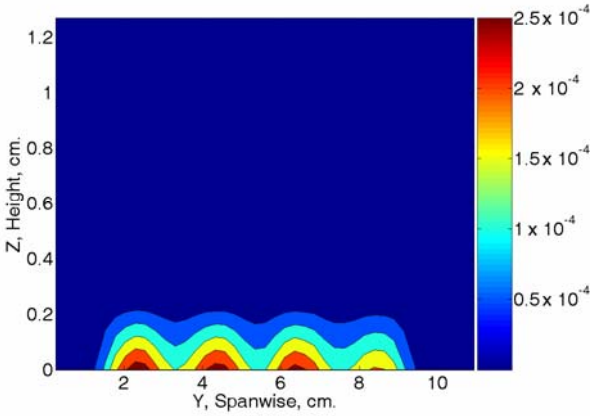


**Figure 4. $I_M$ across a streamwise slice of the flat plate at $x$ = 1.8 cm.**

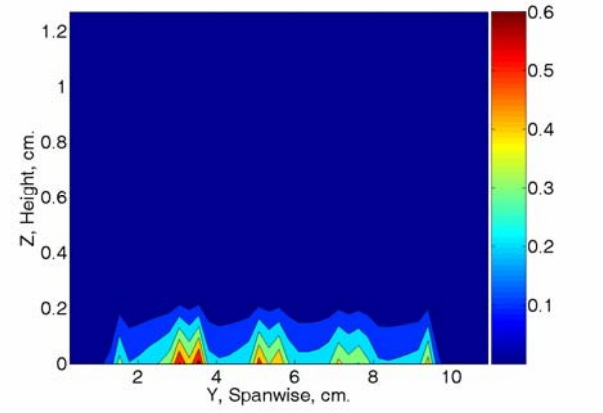


**Figure 5. The modified equation for $I_{EM}$ across a streamwise slice of the flat plate at $x$ = 1.8 cm.**

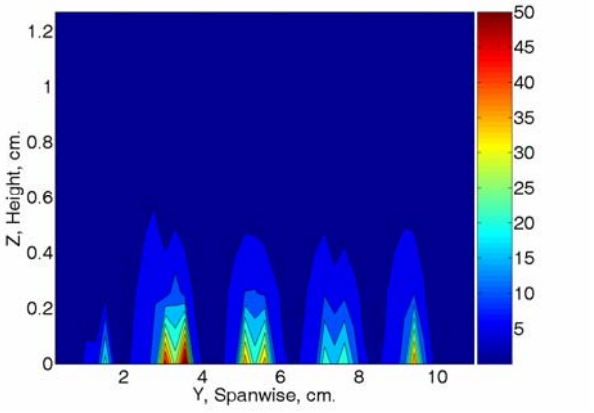


**Figure 6. 20 kV EHD body force (N/m$^2$) across a flat plate streamwise slice at $x$ = 1.8 cm.**

significantly with height, but remains viable for boundary layer applications. Figure 3 shows that the force is greatest over the electrodes, especially at the edges where the maximum charge is located. The Lorentz force is not as high over the outer electrodes because the electric field terminates after reaching ground. As Fig. 4 shows, the magnetic interaction parameter is very low, with values no higher than $2.5 \times 10^{-4}$. Without accounting for the reduction in velocity in the boundary layer, the values of $I_M$ would be even lower. However, $I_M$ can be manipulated by multiplying it by another dimensionless quantity, $E/Bu_{BL}$, yielding

$$I_{EM} = \frac{BE\sigma L}{\rho u_{BL}^2}. \tag{14}$$

As Eq. (14) shows, the electric field becomes a variable in this parameter, and the expression for dynamic pressure exists in the denominator. Therefore, Eq. (14) may be distinguished as the electromagnetic interaction parameter. The values are much higher near to the plate for this modified parameter, but the magnitude drops off significantly with height, reaching values of $10^{-7}$ in the upper corner regions of Fig. 5.

A review of the data used to produce the figures above shows that $EB >> u_{BL}B^2$ in Eq. (12). Therefore, the ratio of the EHD and MHD body forces can be simplified for many $B < 1$ T, boundary layer EMFC cases to

$$\frac{F_{EHD}}{F_{MHD}} \approx \frac{\varepsilon_0 E}{\sigma BL}. \tag{15}$$

Equation (15) shows that the MHD body force is approximately five orders of magnitude larger than the EHD body force shown in Fig. 6 across the entire flat plate. This result is shown in Fig. 7. However, one must remember that the EHD body force is created with an electrode potential of 100 V for the example actuator. The 1.59 cm electrode gap will allow up to a potential of roughly 20 kVDC at atmospheric pressure, which would result in a glow discharge[21,22] and the highest Coulomb force before electrical breakdown. Figure 6 shows this 20 kV body force, which can be compared to the results of Fig. 3. For the calculation, $L$ was removed from Eq. (10) to give the body force units of $N/m^2$ to match with Fig. 3. (Also, note that for the EHD body force to be applied in the same direction as the MHD body force, the electrodes would have to be switched so one was upstream of the other.) Finally, Eq. (15) can be expanded to allow for a direct comparison between forces created with different EHD and MHD electrode potentials. Figure 8 charts the results of this modified equation for the 20 kV EHD electrode potential case.

$$\frac{F_{EHD}}{F_{MHD}} \approx \frac{\varepsilon_0 E_{EHD}^2}{\sigma E_{MHD} BL} \tag{16}$$

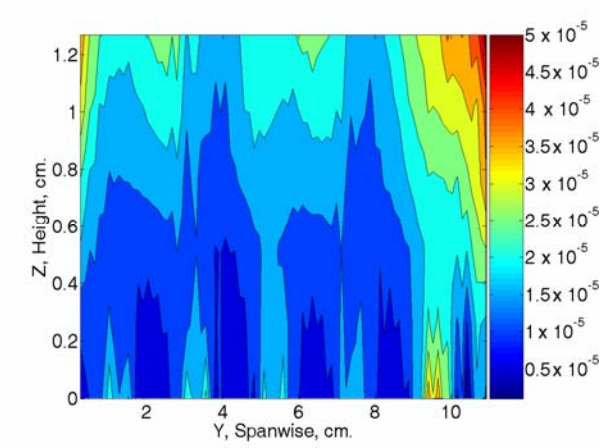


**Figure 7. Equation (15) plotted across a streamwise slice of the flat plate at $x$ = 1.8 cm, 100 V (MHD) vs. 100 V (EFC) case.**

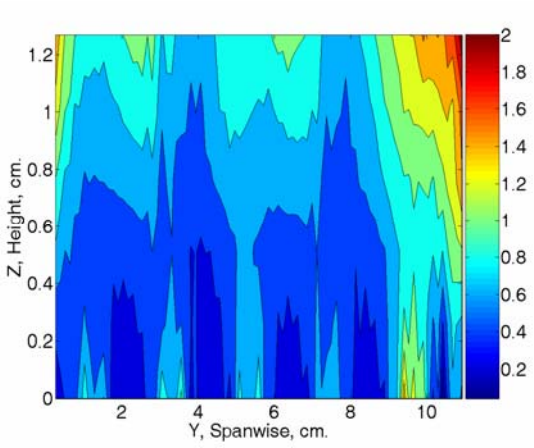


**Figure 8. Equation (16) plotted across a streamwise slice of the flat plate at $x$ = 1.8 cm, 100 V (MHD) vs. 20 kV (EFC) case.**

As one can see from Fig. 8, the Coulomb force for the 20 kV EHD electrode case is generally still less powerful than the Lorentz force produced by an electrode potential of 100 V, σ = 1 mho/m and the same electrode gap width. The Coulomb force is only greater than the Lorentz force very near to the electrodes, or very far from the flat plate where each force is negligible compared to the dynamic pressure. Also, the Coulomb force drops faster than the Lorentz force between the electrodes. An important observation to make from Fig. 8 is that, while the Coulomb force cannot be raised due to electrical breakdown limits, the Lorentz force could still be significantly increased by raising $\sigma$, raising the electrode potential, or by increasing the streamwise length of the electrodes.

Continuing on, the magnetic Reynolds number is a measure of the ease with which an ionized gas moves through a magnetic field, and is defined as

$$Re_M = \mu_0 \sigma u L. \tag{17}$$

It is well known that the motion of charged particles in a current field can create an induced magnetic field $b$, responsible for many phenomena in space. A relationship between the magnetic Reynolds number, the current field, and the induced magnetic field is

$$Re_M J = \nabla \times b. \tag{18}$$

Using the aforementioned ranges of $\sigma$, $u$ and $L$, the $Re_M$ is very low within the boundary layer and a very high current field is needed for an appreciable value of $b$. Therefore for EMFC actuators, $b$ may indeed be negligible.

Going back to Eq. (13), it does not appear that reaching $I_M \approx 1$ is feasible for EMFC devices similar to the one shown in the preceding example. Perhaps other dimensionless numbers are available to quantify the electromagnetic force required for control. With pressure changes often measured to confirm the effect of the Lorentz force, variables to consider include $B$, $E$, $\sigma$, $p$, $u$, $L$, and $\rho$. Table 1 below shows several resulting dimensionless numbers.

**Table 1. Resulting Dimensionless Numbers for Several EMFC Variable Combinations**

| Variable Combinations | Dimensionless Numbers |
|---|---|
| $B, E, \sigma, u, p$ | $\frac{E}{Bu}$ |
| $B, E, \sigma, u, \rho$ | $\frac{E}{Bu}$ |
| $B, E, \sigma, L, p$ | $\frac{BE\sigma L}{p}$ |
| $B, E, \sigma, L, \rho$ | $\frac{E\rho}{B^3\sigma L}$ |
| $B, E, \sigma, L, p, u$ | $\frac{E}{Bu}; \frac{BE\sigma L}{p}$ |
| $B, E, \sigma, L, \rho, u$ | $\frac{E}{Bu}; \frac{\sigma B^2 L}{\rho u} \rightarrow \frac{BE\sigma L}{\rho u^2}$ |

As one can see, the results do not immediately point to a new useful scaling parameter. The last row shows the creation of $I_{EM}$ as shown in Fig. 5. Removing $u$ from the variable combinations leads to some interesting parameters, but it is difficult to see any significance based on limited EMFC results. Another modified interaction parameter has been discussed,[12,23-25] and it is written as

$$I_{BL} = \frac{\sigma B^2 L}{\rho u_\infty \sqrt{c_f / 2}}. \tag{19}$$

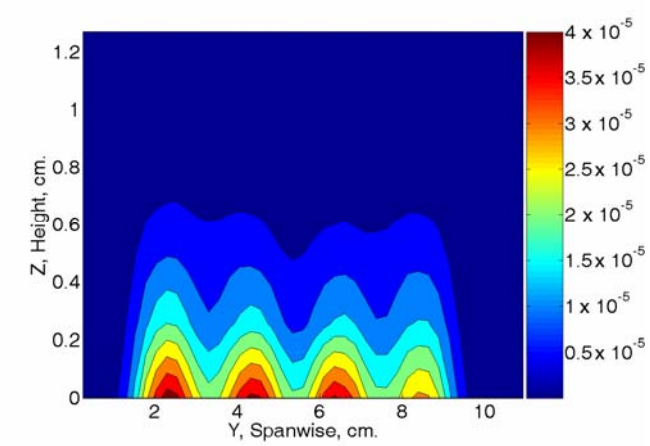


**Figure 9. $I_{BL}$ across a streamwise slice of the flat plate at $x$ = 1.8 cm.**

Figure 9 shows $I_{BL}$ graphed for the same geometry and conditions as the example EMFC actuator presented in Section II. For Fig. 9, the value of $c_f/2$ is approximated as $2.0 \times 10^{-3}$. Here, the values are actually lower than those of Fig. 4 using Eq. (13). This is because the freestream velocity $u_\infty$ = 1000 m/s is used for generating Fig. 7 while the other figures use the local boundary layer velocity $u_{BL} = u(z)$. If $u_\infty$ is fixed at 1000 m/s for each model, then $I_{BL} >> I_M$. Drawing conclusions, it appears that $I_{BL}$ may be more appropriate for EMFC than $I_M$ since it provides proper scaling for boundary layer phenomena. However, $I_{EM}$ may also be a significant parameter. Desirable aspects of it include the inclusion of $E$ and a direct comparison of electromagnetic forces and dynamic pressure. Its value is near unity under atmospheric conditions and moderate values of $E$, $\sigma$ and $B$. Also, $I_{EM}$ follows similar geometric contours when compared to the Lorentz force calculated for the example actuator. This similarity should be beneficial for designing and characterizing EMFC actuators in the design space where $EB >> uB^2$, which may be significant.

Also of importance to a discussion of scaling parameters and the difference between electric and electromagnetic forces is the interaction parameter for EHD,[25] written as

$$Z_{EHD} = \frac{\varepsilon_0 E^2}{2\rho u^2}. \tag{20}$$

Like $I_{EM}$, this parameter involves dynamic pressure in the denominator. Interestingly, dividing the term above by $I_{EM}$ leads back to the $F_{EHD}/F_{MHD}$ ratio expressed in Eq. (15).

## III. Issues with Designing an Electromagnetic Flow Control Surface Actuator

For electromagnetic fields to be successfully applied into a control surface actuator, several issues must be considered. First, while channel flow setups are ideal for understanding the physics of EMFC, open flow experiments must be considered in which the EMFC actuator is contained in a flat plate or airfoil. Power consumption and packaging are important issues to address, with the selection of magnets and the method of ionization key to success. The selection of EMFC magnets is a significant matter since rare-earth materials would be ideal for placement inside a thin control surface, except for the major problem in which their field strength is adversely affected by heat. Finally, unlike EFC, a sufficiently high value of conductivity must be created by an additional system in which thermal ionization is not encountered in the flight regime chosen.

### A. Channel Flow and Open Flow Experimentation

While one of the focal points of EFC has been for control surfaces, the same cannot necessarily be said for EMFC systems thus far. EMFC experiments applied to aerospace systems have typically been for scramjet systems and have taken place in a channel flow environment. Analytical approaches have also been well established for MHD channel flows (e.g., Ref. 26). One current channel flow system has been configured to place an accelerating or retarding force on a high-speed flow (Mach 3.0-4.0) of air or another mixture of gases.[12,23,27-37] The test section pressure is limited to 7-20 torr.[27] The gas is transformed into a weakly ionized gas (WIG) by means of a high voltage, high frequency electric field pulse circuit. A dedicated DC power supply provides the energy for the Lorentz force effect. The channel itself is small enough to be surrounded with an electromagnet, while a rare earth magnet configuration has also been demonstrated.[29]

A similar channel flow test section has been built that has a Mach number of 2.8 and static pressure up to 28 torr.[38] In the test section, two electrodes are placed on the side of one of the tunnel walls. A helium-cooled superconducting ring magnet surrounds the channel and can generate a field up to 7 T.[39] Instead of two separate power supplies for ionization and Lorentz force generation, a single 20 kV, high current regulated power supply is

used. The electric field generated by the 20 kV potential ionizes the gas to the point of breakdown, and the resulting arc draws up to a specified current limit. Once the current limit is reached, the power supply voltage drops significantly, so the power input into the flow is considerably less than 20 kW. Therefore, the initial 20 kV potential before breakdown acts like an ignition system for the EMFC actuator.

Another channel flow facility has been developed with a flat plate secured inside a free jet test section. The Mach number in this facility is about 5.0, and the test section static pressure is designed to simulate an altitude between 30 and 50 km (approximately 0.6–7 torr).[40] Besides covering the altitude range mentioned, the low test section pressure has also been designed with consideration to raising the value of $I_M$. Although the electrodes are arranged on the surface of the flat plate, an electromagnet with a maximum field of 3.5 T surrounds the entire channel. Also, an array of NdFeB magnets can reach 0.5 T. Total lift and drag measurements can be made on the plate.[41] A WIG is generated with either a DC electrical discharge, RF radiation, or with both acting together. The WIG conductivity can reach about 2 mho/m. The DC discharge is diffuse at 400 V with a current up to 550 mA.

All of these facilities are similar in that a low temperature WIG is generated and then manipulated by an EMFC actuator. These ionization systems and the overall electrode design for the simultaneous manipulation of the WIG appear to be feasible for high-speed, boundary layer EMFC based on earlier results from these facilities. However, the value of conductivity generated (0.1–2.0 mho/m) by the high voltage systems as well as the test section pressure (7–20 torr[27]) are several orders of magnitude below those that may be necessary for the AJAX engine concept. It would be very interesting to modify the geometry and examine the performance of these systems under an open flow, flat plate environment with pressures closer to what may be encountered by a wing or fin during high-speed flight. Magnets should also be embedded in the surface. Control of slender wings and fins, and perhaps the initial stage of an inlet compression system, are probably the best applications for these systems. If changing the geometry and increasing $p$ are not formidable obstacles, perhaps these types of systems could be placed on a high-speed missile for control purposes.

Typically, one or more transducer ports are placed downstream of the electromagnetic arrangement to capture the experimental change in static pressure resulting from the Lorentz force. Figure 10 shows an example of the resulting normalized pressure change when the EMFC system is activated for a little less than one second.[35] The pressure shift is higher when the Lorentz force acts against the flow direction. Another measurement often seen with salt water-based EMFC or EFC is the change in boundary layer profile relative to the free stream velocity and actuator power input. Since salt water is naturally conductive (a few mho/m), flat plate Lorentz force actuators have been much easier to build, test, and characterize.[24,42] Note that Ref. 24 discusses an interaction parameter similar to $I_{EM}$. Figure 11 shows the change in boundary layer profile for a low-speed salt water freestream flow of about 18 mm/s as measured with a PIV system. Hopefully, new research into EMFC with air will be able to measure changes in the boundary layer velocity profile. The inherent non-uniformity of the Lorentz force field probably adds unusual effects that must be measured as a function of height above the plate as well as in the spanwise direction.

Although the flow speed in Fig. 11 is very low, the concept of electromagnetic flow control and propulsion for naval applications has existed just as long as it has for aircraft.[43] The concept has also been proven with subscale submarines and ships.[44,45] Studies of MHD propulsion have concluded that

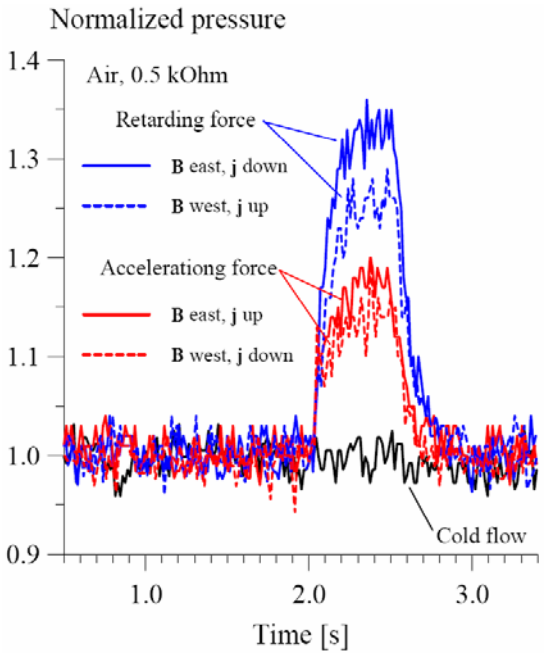


**Figure 10. Normalized static pressure traces downstream of an EMFC actuator for M = 3 dry air for four electromagnetic arrangements (from Ref. 35).**

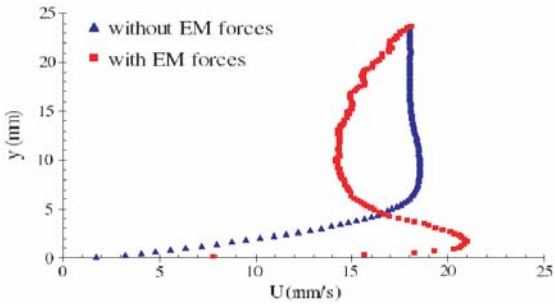


**Figure 11. Boundary layer velocity profile downstream of a flat plate EMFC actuator for salt water flow (from Ref. 42).**

MHD propulsion is feasible and desirable because of stealth.[46] However, MHD propulsion for a full-scale submarine will require significant power and new developments in efficiency for an on-board nuclear reactor.

### B. Power Consumption and Packaging

For EFC systems, power consumption and packaging are relatively simple issues. Glow discharges require high voltage, but they are generally low power phenomena. Dielectric barrier discharges (DBDs) also require high voltage, but the low current requirement again leads to low power consumption. Corke and Post report a power level of approximately 6.5 to 130 W per spanwise linear meter of the actuator.[47] Since the actuators are often thin in the streamwise direction, the power requirement is anywhere between several hundred watts and a few kilowatts per square meter of a hypothetical control surface. Assuming that DBD systems are capable of manipulating high-speed flows, the power consumption is probably low enough for integration into a flight vehicle or missile. Since glow discharge and DBD systems often use small, thin sets of electrodes, packaging is also straightforward. Figure 12 shows the ease at which these actuators can be placed onto a surface as long as the material they are embedded in is dielectric.[48] The largest components of these systems are the high voltage elements, but the overall mass of these systems is constantly decreasing with improvements in electronics. The thrust from these DBD arrangements rises with the dissipated power.[49] Assuming the thrust for high-speed actuators will need to be higher than those that currently accelerate a flow by a few meters per second, they will have significantly higher power consumption than what was reported in Ref. 47.

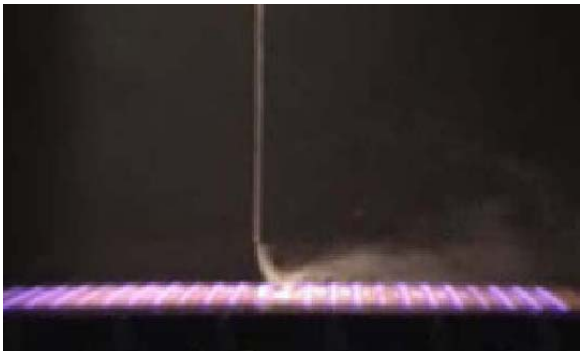

**Figure 12. Smoke visualization of a DBD control surface composed of rows of actuators creating an electrostatic force that acts from left to right (from Ref. 48).**

Concerning EMFC systems, the packaging issue is more complex and dependent on the choice of magnets. Figure 13 shows a large electromagnet surrounding a hypersonic test section.[41] Figure 14 shows the five electrode, four NdFeB magnet actuator previously discussed. The configuration of Fig. 14, whether composed of rare earth magnets or small electromagnets, looks to be the most compact method of placing an EMFC actuator on the surface of a wing or at the beginning of an inlet compression system. The obvious drawback of efficient packaging with embedded magnets is the relative reduction in magnetic field strength across the control surface. However, going back to the discussion of $I_{EM}$, the reduced $B$ field can be offset in the interaction parameter with a higher electrode potential.

Even if the EMFC actuators themselves are compact, the power consumption will create the need for a large

**Figure 13. A water-cooled electromagnet surrounds an EMFC free jet test section (from Ref. 41).**

**Figure 14. An EMFC actuator with a 10.8 × 3.2 cm surface area and embedded NdFeB magnets.**

generator. Perhaps a short duration air-to-air missile (with EMFC actuators for rapid course corrections) could operate based off a power supply equivalent to a few batteries typical of current missile technology, but longer missions will require innovation. MEMS microturbine generators may someday be able to generate the level of power needed while weighing significantly less. The exact power consumption of effective high speed EMFC systems is still relatively unknown. An ionization system also may require a power supply that is separated from the Lorentz force actuator. However, it appears that the power requirements for ionization by an electric field will not be particularly detrimental as the high voltage pulses have a low duty cycle and are created from a modest power supply.[28]

### C. Selection of EMFC Magnets

The selection of appropriate magnets for electromagnetic flow control systems is a current topic of debate. Electromagnets have seen the most use in MHD experimentation. However, the advancements in several new rare earth magnetic alloys between 1970 and 2000 has made permanent magnets viable for aerospace applications of magnetohydrodynamics.[50] Permanent magnets, where possible, should be considered instead of electromagnets since they consume no power and demonstrate much higher values of energy density making their strength-to-weight ratio relatively superior. Unfortunately, the main drawback of using permanent magnets for aerospace applications is the fact that high temperatures drastically weaken their overall surface field strength. Permanent magnets lose their magnetic properties at a specified point called the Curie temperature. Prior to that point there is another temperature called the maximum operating point, after which a magnet will experience permanent losses to its original strength.[51] For AJAX-style scramjet engines, it is unlikely that permanent magnets could be used in the high temperature environments even with complex active cooling systems. Another drawback to rare earth magnets is their handling and safety. Other industries that have implemented rare earth magnets into products experienced early troubles with assembly because of their surprisingly strong pull force.[52] However, it is possible to incorporate the magnets into an assembly before magnetizing them.

Figure 15 shows the maximum operational temperatures of samarium-cobalt and neodymium magnets charted along with typical post-shock temperature curves as a function of Mach number for different wedge angles with an incoming stream at 220 K. Neodymium magnets are operationally limited to temperatures just over 400 K, while some samarium-cobalt alloys can be used at temperatures exceeding 800 K. While these temperatures are still far below the requirements of implementation into a multi-shock scramjet inlet, these magnets could be used for slender control surfaces to some extent on supersonic and hypersonic missiles or vehicles. Moreover, while it would appear that samarium-cobalt is superior to neodymium for high-speed aerodynamic control, Fig. 16 shows that the high-temperature alloys typically will see a large reduction in magnetic field strength when compared to their lower temperature versions.[53] Note that the magnetic flux density is measured using teslas, but the values from Fig. 16 are not representative of the maximum magnetic field (also measured in teslas) that will be present on the surface of the magnets. Neodymium and samarium-cobalt magnets are widely available, but they rarely demonstrate maximum surface fields over 0.5 T. Figure 17 shows that it is common for permanent magnets to lose the bulk of their surface field before reaching their maximum operational temperatures.[54] Typically, these magnets will see a slight linear decline in surface field for a limited temperature range before reaching a point of rapid decline extending to the maximum service temperature. One of the focal points of current research in magnet development has been to broaden the temperature range in which only a slight linear decline is present, with significant improvements made to samarium-cobalt alloys[55-58] and apparently little work carried out with neodymium alloys. As far as the surface field is concerned, one can conclude that neodymium magnets are a better choice for applications with temperatures ranging up to 350–400 K. However,

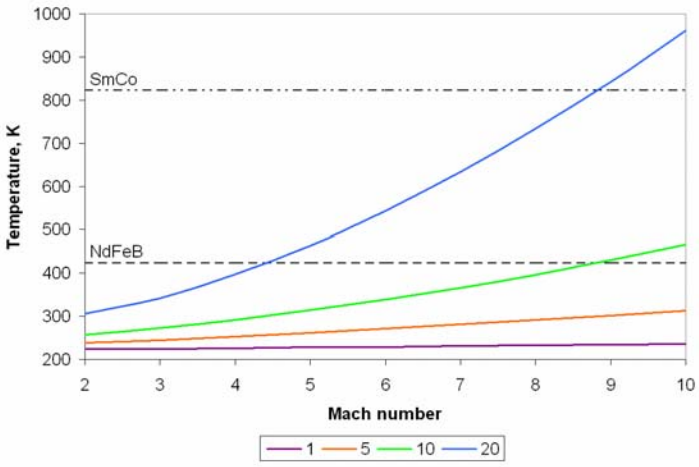


**Figure 15. Temperature versus Mach number for lines of constant wedge angle (1°, 5°, 10°, 20°) after an oblique shock wave (based on an initial temperature of 220 K).**

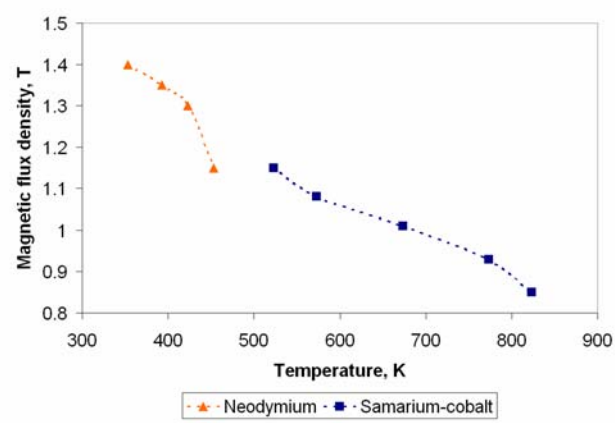


**Figure 16. Magnetic flux density charted as a function of the maximum operating temperature for several neodymium and samarium-cobalt alloys.[53]**

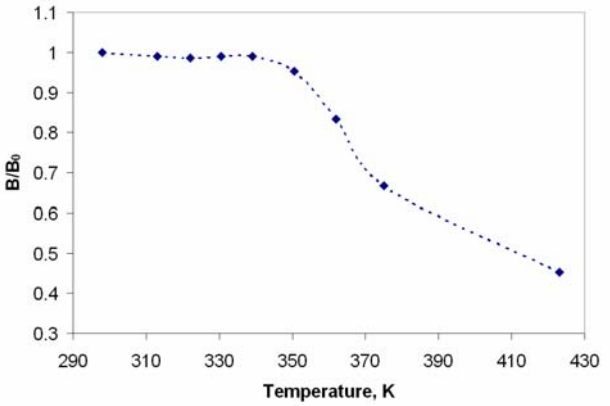


**Figure 17. A typical plot of the surface field decline versus temperature for a neodymium magnet with a maximum operating temperature of 423 K.[54]**

the typical decline of the neodymium surface field as shown in Fig. 17 indicates that samarium-cobalt magnets will be superior after the 400 K point.

Concerning the viability of electromagnetic flow control, an inquiry must be made to understand exactly what range of magnetic surface field values is needed. This question leads back to the reason why magnets are needed for EMFC in the first place, namely, that the cross product of magnetic field and the electric field produces the Lorentz force. Even more fundamental, the presence of a magnetic field acts as a facilitator for energy addition into the fluid flow from the electrodes. The energy addition is then, of course, split into joule heating and the kinetic energy (rate of work done by the Lorentz force) of the fluid. If only a few kilowatts of power are needed for effective electromagnetic flow control and $\sigma$ is in the range of 0.1–1.0 mho/m, then using NdFeB magnets is practical with electrode potentials of a few hundred volts or less. As was mentioned previously, many recent experimental EMFC facilities have used powerful electromagnets capable of surrounding a test section since it is a straightforward way to increase the magnetic interaction parameter. However, some of these ring-shaped electromagnets have masses of hundreds of kilograms[39] which makes flight applications problematic. Thus, a trend towards using permanent magnets for aerospace applications has started, with at least a mention of them in several recent publications.[20,24,29,40,42,59,60] Obviously, conductivity is another facilitator for energy addition into the flow. The concept of low temperature, conductive particle seeding[59] could also lessen the need for powerful (>1 T) magnetic fields, as long as the seeding does not obstruct or adversely contaminate the flow.

### D. Conductivity

In 1968, Garrison stated that the performance of MHD accelerators depends directly upon the magnitude of the electrical conductivity of the seeded working gas.[61] Before then, the concept of propulsion using electric and magnetic fields had appeared in the literature for several decades.[62-67] Efforts at experimentation began in the late 1950's beginning with the implementation of plasma jets for propulsion systems.[68] Plasma jets were certainly capable of generating highly conductive gases through thermal ionization, but the temperature and power requirements were too high for viable aerospace applications at the time. Alkali salt seeding was therefore introduced into the plasma jet in order to achieve the same level of conductivity at a considerably lower temperature.[3] Extensive experimentation with different seed materials and gases appeared in the literature[69-80] through the end of the 1960's, with conductivities up to 1000 mho/m achieved. The experimental gas pressures reported were usually on the order of 1 atm. At higher pressures (e.g., 10 atm), electron attachment by positive oxygen atoms significantly reduces $\sigma$.[81]

Like many other fields, research in magnetohydrodynamics was affected by the direction of the Apollo program. It appears that engineers may have assumed that megawatts of power produced by an onboard nuclear reactor would be available for future MHD accelerator-based propulsion systems, but the nuclear prospect never materialized with the exception of the Project Pluto engine testing program.[82] Additionally, the success of controlled ablation reduced the need for further research into electromagnetic flow control for use on re-entry capsules.[83] Arc jets were then applied to ground testing systems with many integrated into wind tunnels as a source of high enthalpy, high velocity

flow.[6] Seeding is still a viable method for increasing the performance of those wind tunnels, but it can lead to undesirable contamination of the flow.[84] This series of events effectively halted the prospects for MHD systems for aerospace vehicles. Power generation[85,86] became almost the sole focus of MHD research, with the exception of the submarine development previously mentioned. Despite the fact that electric engines make use of a comparatively weaker force, electric propulsion[87] developed simultaneously with MHD propulsion and eventually flourished due to a low enough power consumption to be used with emerging radioisotope thermoelectric generator technology.[88]

The past decade has certainly seen a reemergence of MHD research applied to aerodynamics. Obviously, the history above shows that generating and controlling a flow with $\sigma > 100$ mho/m is difficult because of the power requirements. Creating ionization from a thermal source such as a plasma jet is not desirable, and is probably not possible for aerodynamic control surfaces. Ionization can also be achieved through high voltage fields, laser beams, microwaves, and radiation - indeed any method of transferring energy to cause molecular excitation of the gas. Of the EMFC facilities mentioned thus far, all have at minimum employed high voltage fields. However, there is a difference between each on how the high voltage fields are applied.

Perhaps the easiest method of creating plasma with a voltage field is to apply a large potential difference between two electrodes. Based on factors like separation distance, voltage, geometry, and the gap material, a plasma column (also noted as an arc discharge) will form between the electrodes. The current is based on the effective resistance of the gap. When the plasma column fills the gap with electrons, the resistance is immediately lowered and the potential current that can cross the gap is large enough to create the need to stabilize it with a high power load resistor. To create a plasma column, Zaidi et al. used this principle and operated in a constant current, variable voltage mode.[38] The power supply potential was 20 kVDC, and the maximum current was 1 A. Fixing the current to, for instance, 1 A and activating the power supply causes a high voltage field to be applied until electrical breakdown occurs and a plasma column forms. Once the column forms, the voltage required to maintain a 1 A current can be very low. During the wind tunnel experiments, the plasma column that forms between the electrodes was found to be periodic with a frequency of 1–10 kHz. Once a plasma column forms between the path of least resistance, it travels downstream where the gap between the electrodes gradually increases similar to a Jacob's ladder. While applying a 1.7 kV field at 35 mA with no magnetic field, the plasma column traveled downstream at 360 m/s. When a magnetic field of $B = 2.0$ T is applied, the column speed increased to 2000 m/s.[89] With this electromagnetic effect, some control of boundary layer separation created by an oblique shock over a wedge was demonstrated.[90] Perhaps the plasma column speed can be increased with a refined geometry and different applied voltages and currents to increase the control. However, one problem with the generation of plasma columns is their destructive behavior. To operate with higher power, an assembly consisting of a sapphire base plate and high temperature arc corrosion-resistant electrodes was constructed.[89]

The other DC ionization system previously mentioned was originally discussed by Shang et al. in 2002 as part of an EMFC actuator aimed at affecting the shock wave structure around a blunt body.[91] Differing from the work of Zaidi et al., a diffuse WIG is created instead of a plasma column due to a lower applied voltage and a lower static pressure. Also, the electrode geometry plays a significant role in transitioning from a diffuse glow to an arc. The blunt body was replaced with a flat plate made of a ceramic base and two embedded copper electrodes.[92] Figure 18 shows these electrodes, with the upstream cathode experiencing a much more intense glow.[93] This diffuse glow discharge begins to constrict and transition to an arc when the current surpasses 100 mA or when $B$ is greater than 0.2 T.[94] A pulsed signal with a frequency between 5 Hz and 10 kHz was also used to explore the response of the Mach 5 flow to the actuation of the electromagnetic field.[95] Furthermore, RF radiation was added to augment the ionization created by the DC glow discharge, resulting in a reduction in the impedance across the electrode gap.[96] Accounting for all of the ionization

**Figure 18. A DC voltage discharge between two electrodes at freestream conditions of M = 5.15 and $p$ = 0.59 torr. The applied voltage is 880-920 V at a current of 50 mA. The addition of a magnetic field significantly affects the plasma and creates a virtual hypersonic leading edge strake (from Ref. 93).**

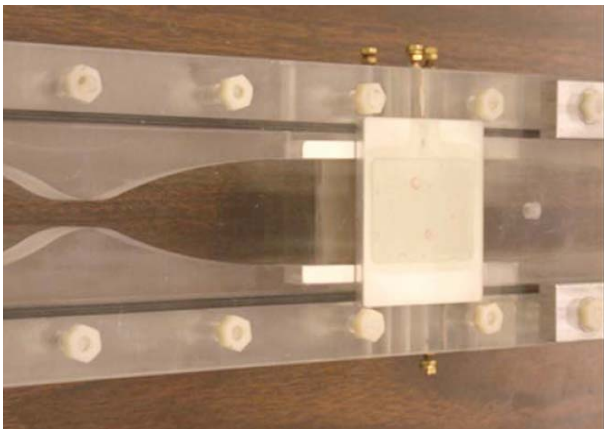

**Figure 19. EMFC test section with magnet removed to show the electrode placement. The back of one of the RF WIG generator electrodes appears on the side with the DC Lorentz force electrodes mounted on the top and bottom. (from Ref. 27).**

methods, the maximum power requirement remained a few kilowatts or less and can result in a conductivity of a few mho/m in a low pressure environment. The research presented in the various publications for this facility certainly shows that a DC voltage discharge combined with a magnetic field can produce enough of a force to significantly affect a boundary layer at hypersonic speeds. Such results are very promising. However, DC discharges do not easily remain diffuse at higher pressures.[21]

A wide variety of research has shown that the degree of ionization produced by an electric field is higher for pulsed discharges rather than for a steady DC discharge. Pulsed discharges simply can withstand a higher applied electric field (and more power) before a transition to arcing occurs.[97] However, the applied Lorentz force should be continuous and therefore should be generated with a DC power supply. Palm et al. addressed these issues by creating an EMFC channel facility with RF WIG generation and simultaneous DC Lorentz force application.[12] The test section is shown in Figure 19 with the nozzle appearing on the left side of the picture. The facility generated a diffuse WIG for Mach 2–4 flow originally by using a 13.56 MHz, 600 W RF power supply.[29] Conductivity (0.1–1.0 mho/m) scales with the power draw of the system. Since that time, a more complex ionization system has been constructed to raise the attainable level of conductivity without raising the power draw. Meyer et al. first reported using this system to attain $\sigma \approx 0.1$ mho/m in a Mach 4 flow by compressing a 500 V, 1 μs pulse into a high frequency (up to 50 kHz), high peak voltage (20 kV), short duration pulse (10–20 ns).[32] During the peak voltage application, the current reaches 90–100 A, but the short duty cycle results in reasonable overall power consumption. According to Nishihara et al., raising the frequency of the system from 40 kHz to 50 kHz increases the flow conductivity along with lowering the ballast resistance.[34] It would be interesting to see a parametric study of the flow conductivity as a function of the pulse frequency. The point of using such a high frequency is to counteract the rapid decay of the WIG. The life of the WIG can be observed by measuring the current draw from the DC

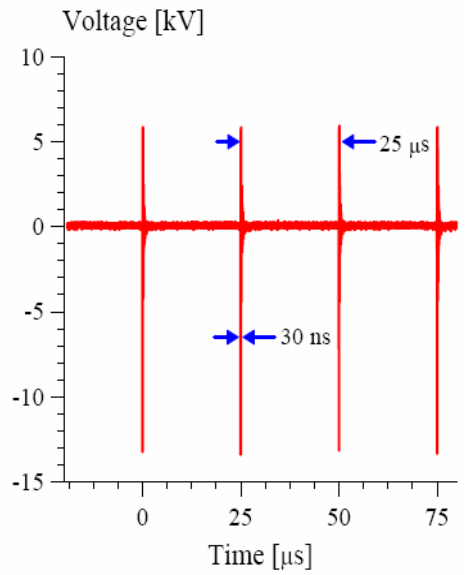


**Figure 20. Voltage oscillogram for 40 kHz pulsed ionization of a Mach 3 nitrogen flow. The test section pressure is 8.4 torr and *B* = 1.5 T (from Ref. 36).**

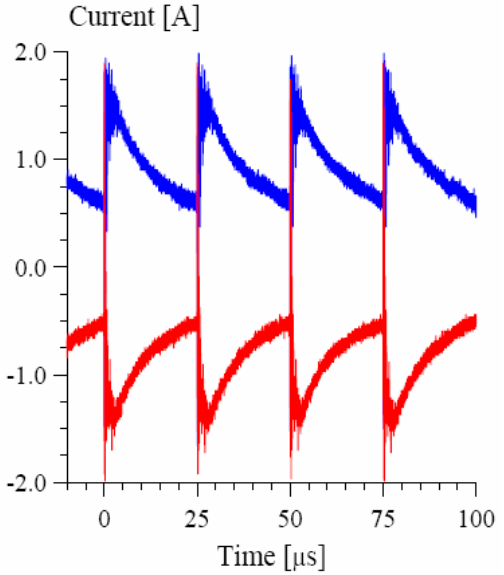


**Figure 21. Current oscillogram for Lorentz force power supply with the test conditions of Fig. 20 and different 2 kV electrode polarities (from Ref. 36).**

Lorentz force power supply. Figure 20 shows four pulses measured from the ionization system operating at 40 kHz. Figure 21 shows two current oscillograms measured from the DC Lorentz force circuit for the same conditions as Fig. 20, created with constant electrode potentials of 2 kV (one at each polarity). The current rises at the initiation of each ionization pulse, and then falls with the WIG decay. With slightly different test section conditions, a current oscillogram appears in Ref. 37 for an ionization frequency of 100 kHz, which results in a steadier Lorentz force because the WIG decays less. As one can see from Fig. 21, the Lorentz force system has an average power consumption of about 2 kW and it is capable of creating the pressure changes shown in Fig. 10.

### E. Overall Feasibility

A few examples of recent EMFC facilities have been presented in this section. These facilities have emphasized electromagnetic forces within the boundary layer and they have shown that EMFC can have a considerable effect at supersonic and hypersonic flow speeds. However, the pressures at which these experiments have been conducted, as well as the magnitudes of $\sigma$ and $B$, are far below what may be necessary for a hypothetical AJAX scramjet engine. As such, these systems are more applicable for boundary-layer control of an aerodynamic surface. Several steps must be taken to transition to a feasible electromagnetic virtual control surface. Experimental facilities have demonstrated success using low pressure core flows often surrounded by large magnets, and it is time to consider more compact configurations that can simulate external flow over a wing or the beginning of an inlet compression system. In these environments, the magnets can be embedded below and between the electrodes. Novel cooling methods must be developed for permanent magnets to survive the high-temperature environment. EMFC actuators may be placed in regions where the surface is actively cooled or is relatively cool. Test section pressures must be increased, not necessarily to atmospheric, but perhaps to simulate the pressure after a shock over a thin wedge. The Mach 5 EMFC facility test section pressure reported by Shang et al. was meant to simulate an altitude from 30-50 km (0.6–7 torr),[40] but accounting for a real flight vehicle and a bow shock leads to much higher pressures in that altitude range (for example, a 10° wedge at that speed would lead to a static pressure of 2–20 torr).

Although it appears challenging, experimental generation of a Lorentz force is not particularly difficult for EMFC actuators. The key problem is creating non-thermal ionization to supply a conductive working fluid for the actuator. At low pressures, DC ionization systems are capable of creating a diffuse WIG for which $\sigma$ can reach a few mho/m at high speeds. Control has also been demonstrated with such plasma columns. As pressure rises, the voltage required to sustain a glow discharge rises. This relationship makes arcing for DC discharges more probable if EMFC test section pressures are going to trend higher. High-voltage, high-frequency pulsed ionization sources are another available method for creating the same value of conductivity. Since pulsed discharges can be applied in systems with relatively higher power consumption that are less susceptible to arcing, ionization sources for EMFC actuators should trend towards using RF or square wave signals. Fridman et al. postulate for an electrode gap that voltage pulses of less than about 100 ns per centimeter of anode and cathode separation can sustain streamers without transformation into arcs.[97] Refining that estimate and determining the plasma decay rate between pulses will allow for the optimization of the ionization source and will minimize fluctuations to the flow conductivity. The constant development of power semiconductors should make high-frequency pulsing systems more cost effective. Separate ionization and Lorentz force power supplies can be combined over the same flat plate electrodes with the use of rectifiers or diodes. With these issues properly addressed, EMFC could potentially be used in place of traditional control surfaces at high altitudes if the flight vehicle can spare room for a power supply that will likely draw several kilowatts or more. Perhaps a tradeoff study could be initiated when a power supply requirement is better known for an effective EMFC actuator.

## IV. Flow Control by Glow Discharge

Although much of the previous discussion has been dedicated to flow control by electric and magnetic fields, it must be noted that considerable interest for flow control with only plasma or electric fields has existed for decades. Techniques for aerodynamic flow control by electric fields can be categorized into glow discharges and dielectric barrier discharges, covered in the next two sections, respectively. A glow discharge is formed across a gap of air or another gas between two electrodes with a difference in electric potential. The presence of a glow discharge is based on factors such as electrode geometry, ambient pressure, the gap medium, and the voltage. The glow discharge essentially means that the gap is filled with free radicals and electrons traveling between the electrodes. As such, the current increases rapidly after initial formation. Increasing the voltage after the glow discharge is formed eventually leads to electrical breakdown and arcing. A diffuse discharge is desirable since it indicates that the WIG effects will be uniform throughout the glow region. Often, experimentation with this phenomenon has occurred in low pressure environments where it is easier to create a diffuse discharge with a relatively low voltage. High pressure glows are

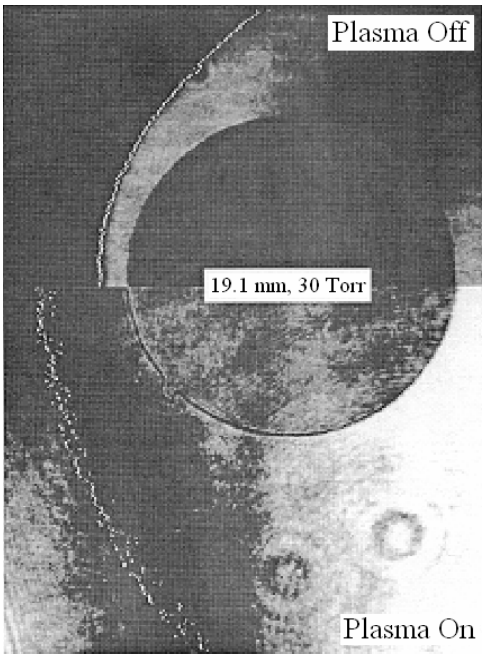


**Figure 22. Split image of a bow shock around a sphere with and without plasma for a flow velocity on the order of 1600 m/s (from Ref. 99).**

also possible, and applying the potential difference with an increasing frequency has shown that the same current is maintained with a lower voltage.[22]

Bletzinger et al. have provided a review of plasmas related to high speed aerodynamics, containing a short history of the development of experimentation with glow discharges.[98] In summary, initial shock tube experiments were conducted by measuring the drag and shock wave structure of objects (often blunt) while recording the differences with and without the actuation of a plasma source. As shown in Fig. 22, plasma flow as opposed to typical flow can drastically change the standoff distance of a bow shock around a blunt body.[99] Similar results were demonstrated as early as 1959 by Ziemer.[100] This is important because a change in standoff distance can reduce heating and drag. Furthermore, the properties of a glow discharge may be used to improve the off-design performance of a high-speed inlet compression system by manipulating the shock wave structure. These features of glow discharges are significant for the future development of re-entry vehicles and hypersonic airbreathing propulsion. Although some of the early shock tube literature makes a case for electrohydrodynamic effects as the reason behind the some of the shock wave alteration,[101-103] the general consensus is that most of the effects seen are a product of the heating from the plasma. Computational studies also indicate this result.[104]

If the bulk of the effects of the glow discharge is from heating, then the next logical step in the process of estimating its feasibility for these applications is to determine if there are benefits of plasma heating as opposed to other sources. Also, one must ask if heating itself can be useful in high speed flight. One benefit of heating by glow discharges when compared to a typical heating element is rapid actuation. This may be a large enough benefit to continue experimentation with surface glow discharges for aerodynamic control. For instance, Shin et al. measured a glow discharge actuation time of less than 220 μs using pin electrodes on a flat plate in a Mach 2.85 flow environment.[105] This flat plate plasma actuator is capable of creating a weak shock wave over the actuator when the plasma is diffuse. A more constricted plasma formation in that environment, although produced with a higher power, does not have the same shock wave control effect. The difference between plasma heating versus surface resistance heating is noticeable, whereby the plasma has more of a volumetric effect, is not exclusively characterized as typical surface heating.[106] However, flow control by plasma heating may have high speed limitations. As speeds increase, the post-shock air temperature increases exponentially and one can assume the plasma will begin to have less of an effect. Also, a rise in flow speed and pressure will reduce the effect if it is considered to be convective. The power of the plasma source can be raised in order to compensate, but the efficiency of control may be drastically reduced.

Although the presence of plasma can change the structure of a shock wave, it appears that most literature involving inlet compression systems also contains magnetic fields for the full Lorentz force effect. However, some research with only plasma has been reported. For a Mach number of 2 and a flow mixture of nitrogen and helium, a glow discharge yielded a significant change in the oblique shock angle over a wedge.[107] The change in the shock angle indicates a change in the Mach number from 2 to 1.8 due to the plasma heating. The WIG source was located on the walls of the wind tunnel. Since the initial ramps of an inlet compression system are not surrounded by an outer wall (e.g., X-43A design), it would be interesting to see if this effect could be duplicated with a WIG source located entirely on the surface of the wedge. Placing a diffuse plasma source on the tip of a wedge and creating an effect on the oblique shock angle is a logical direction to move in to determine if these systems can be placed on a vehicle. Closely related to that design is the concept of a virtual cowl that can be created by plasma heating.[108,109] However, the plasma source is more likely to be high-energy electron beams or microwaves rather than glow discharges. The heat addition specifically can alter the upstream flowfield in order to reduce the inlet spillage. This concept will require a considerable amount of power to operate, but one must consider that any system with plasma heating would be used only during a (presumably short) transition process by acceleration to the design Mach number. Although most of these system designs are analytical models, some experimental studies have demonstrated the concept.[110]

Concerning drag reduction, an initial study showed that the drag coefficient for a sphere in the presence of a WIG was significantly reduced for subsonic flow.[111] The same experiment for supersonic speeds showed that the drag coefficient was higher using a WIG than with typical airflow. Other plasma sources constructed for drag reduction have proven to be more effective since then. Ganiev et al. reported a reduction in the drag coefficient of about 50% from a subsonic speed to Mach 4 using a plasma jet placed at the tip of a somewhat blunt body.[112] Plasma jets appear to be inefficient for streamlined shapes.[98] At the time of Ref. 112, many other publications also described drag reduction with plasma jets and other forms of focused energy addition. A thorough list of these early publications can be found in Ref. 113. However, the large drag reduction by the plasma jet injection appears to be more directly related to the counterflow jet instead of the thermal effects of the plasma.[114] As was discussed, the use of plasma jets was eventually deemed unrealistic for MHD flight applications in the 1960's. Although many of these current systems have been met with enthusiasm, scaling the power requirements to flight vehicles or missiles may pose insurmountable problems with current technology. Although new publications continue to emerge with different plasma sources and test geometries, very little of it is predominantly different from what was carried out at the beginning of this decade. In order to overcome the skepticism resulting from problems including but not limited to power consumption, scaling, and hypersonic interaction at true flight conditions, the science of plasma control for aerodynamics must transition into realistic systems. If a forward facing plasma jet is viable, then it certainly should be able to be demonstrated on the front of a missile. Perhaps an inlet system can be constructed and ground tested with surface actuators that create or manipulate shock waves to minimize inlet spillage. It is understandable that some of the models of full-scale hypersonic systems have not been constructed due to the cost, but plasma control definitely needs to be better proven experimentally as part of more flight-ready systems.

## V. Flow Control by Dielectric Barrier Discharge

Considering the physics involved, a dielectric barrier discharge is similar to a glow discharge. Where a glow discharge has an air gap, a DBD contains a gap of dielectric material between the anode and cathode. Typical materials like glass, polymers, and ceramics have a much higher resistivity than air, allowing for the electrodes to be placed closer to one another. Closer placement increases the electric field around the electrodes and ultimately raises the Coulomb force in Eq. (10) without the occurrence of electrical breakdown. The dielectric barrier is self-limiting as it prevents charge accumulation over the barrier material to prevent arcing. DBDs have been recognized since the mid-19th century, with the their first application being the production of ozone.[115] Since that time, research has continued to grow and now applications include surface treatment, reduction of pollutants, lasers, and plasma display panels. Systems using glow discharges often use low pressure, but the discharges were stabilized across the barrier at atmospheric pressure beginning in the 1980's.[116]

Dielectric barrier discharges constructed for aerodynamic flow control applications appeared in the literature near the end of the 1990's.[117,118] In the decade since those reports, research into aerodynamic flow control with DBDs has rapidly increased both experimentally and computationally. A number of reviews have been written,[47,119-121] which probably indicates a variety of opinions on their applicability. At low speeds, DBD actuators have a significant effect on boundary layer flow. Figure 23 shows a notable image of flow reattachment made possible by an array of DBD actuators produced by Roth et al.[122] This actuator system works at atmospheric pressure, and has been named the One Atmosphere Uniform Glow Discharge Plasma (OAUGDP™). The ionization is created with a high voltage

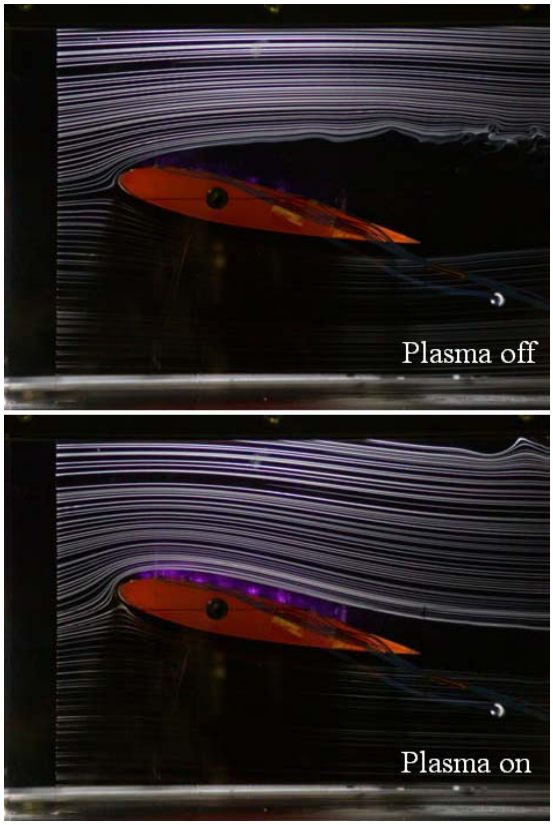


**Figure 23. Smoke visualization shows flow reattachment on a NACA 0015 airfoil at a 12° angle of attack by an array of EFC actuators. The freestream flow speed is 2.6 m/s (from Ref. 122).**

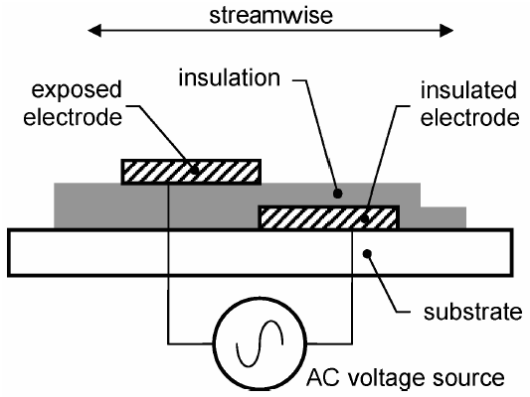


**Figure 24. Typical spanwise cross section geometry of a dielectric barrier discharge actuator for aerodynamics applications (from Ref. 124).**

RF signal and the barrier material is Kapton. Several studies with this system have resulted in successfully increasing or decreasing drag on a flat surface, adding momentum to the boundary layer flow, reducing the boundary layer thickness, and inducing a flow velocity (also known as the ion wind) up to 6 m/s.[123] Figure 23 raises the immediate question about the ability to apply a dielectric barrier discharge system to high-speed flow where flow reattachment, drag reduction, and turbulence suppression are all major concerns. Although DBD actuators are studied by several institutions, the spanwise electrode geometry is always fairly similar and is depicted in Fig. 24.[124]

The relative strength of current systems can be compared by their ability to induce a certain flow speed of air passing over the actuator. The ion wind speed measured in most recent surface DBD actuators is only a few meters per second, and efficient control results are obtained when $u_\infty$ is less than 30 m/s.[119] However, some experiments have been conducted using higher free stream speeds. Opaits et al. investigated DBD control of a NACA 0015 airfoil with free stream speeds of 20 to 75 m/s at atmospheric pressure.[125] The stall angle was raised with the DBD actuators with $u_\infty$ = 75 m/s, and a change in pressure distribution was also recorded. Similarly, Roupassov et al. measured changes in the pressure distribution for a NACA 0015 airfoil at speeds up to 110 m/s.[126] In this case, the electrodes were placed parallel to the flow, and it appears that the pressure distribution incurs a greater change with the DBD actuator when the airfoil is close it its stall angle. One attempt was made recently to mount a DBD actuator on the leading edge of the wing of a Jantar Standard SZD-48-3 sailplane.[127] It appears that the DBD system was able to affect the separation and lift characteristics of the wing surface, but the data were not particularly reliable and refined tests are needed.

In order to maximize DBD actuator performance for high-speed flow control, one may assume that the anode and cathode should have minimal size and be placed as close as possible to each other and separated by a very thin layer of dielectric material. This geometry would maximize the electric field, where the Coulomb force grows with $E^2$ in Eq (10). It has been argued that the force induced from DBD actuators should not be associated with $E^2$ and requires a more detailed analysis.[128] The ion wind is a momentum transfer between neutral particles and heavy ions whose motion is induced by the Coulomb force. As such, the electric field is significantly affected from the charge accumulation and particle interaction over the dielectric gap. Currently, numerical simulations are unable to simulate the observed random microdischarges in time and space that may help to resolve this issue. It appears that the effectiveness of the exposed electrode is increased when it is thinner.[124] However, the ion wind increases with the width of the insulated electrode until it reaches a limit based on the applied voltage. Perhaps new efforts into geometric optimization will yield a viable design for freestream flows of higher speeds. Current systems appear limited in their ability to control high-speed flow, but may be effective on low-speed aircraft. With improvements to their strength, they may become capable of improving the efficiency of turbine or rotor blades as one example.

## VI. Conclusions

Flow control with electric or electromagnetic fields is an exciting topic due to its multidisciplinary nature, the possibility to solve difficult high-speed aerodynamics problems, and the overall design challenges. Also, another long-term factor can be added. It has long been theorized that research into new sources of atomic energy will eventually produce an extremely high power, yet compact generator system. This breakthrough could come tomorrow or hundreds of years from now. When it does come, these new on-board generators will make all forms of MHD flow control realizable. Lorentz force engines may someday replace conventional turbojet and ramjet engines. Actually, the engine tested during Project Pluto shows that a nuclear reactor with 1960's technology was close to being capable of supporting a Lorentz force accelerator with thermal ionization. However, the radiation makes their implementation into a flight vehicle unacceptable.

Rewinding a bit, we must ask ourselves what EFC and EMFC technologies can be supported with on-board power generators with today's technology. Thermal ionization for bulk flows does not appear achievable, leaving the non-thermal WIG sources as the best prospects for creating an appreciable amount of conductivity. Also, the flow speed range in which electromagnetic, glow discharge, and dielectric barrier discharge systems are applicable does

not appear to be clearly defined. EMFC actuators can be characterized in more detail with a better use of dimensionless parameters. For MHD thrusters, reaching $I_M \approx 1$ is achievable. For control surfaces, reaching $I_M \approx 1$ requires extreme low pressures and unrealistic magnetic fields. However, reaching that value may not even be necessary. The parameter defined as $I_{EM}$ may be more appropriate, not just because it results in a higher value, but because it includes the electric field strength. The effects from EFC and EMFC systems should also be able to be compared, and Eq. (16) is a proposed step in that direction that can be developed further with the inclusion of efficiencies and more sophisticated models.

Dielectric barrier discharges, because of their geometric simplicity and compact size, would be ideal for high-speed flow control. For years, their applications have been growing and DBDs can be found in most households and offices in plasma display panels. Additionally, research is continuing to advance their use for surface treatment and reducing pollution. The concept of utilizing DBDs for aerodynamic control has existed for a little more than 10 years. Although this concept is under active research, there is not much variety in the design of these actuators and it appears as though DBDs are limited to freestream flow speeds of less than 30 m/s. Limited control has been seen for speeds over 100 m/s. Therefore, current DBD actuators do not appear to be robust enough for all but very low speed flight applications. The systems may be integrated into UAVs and other small vehicles, but it is unclear if there will be a distinct advantage using this particular control concept. Again, a tradeoff study should be considered for this issue. The power requirement is low enough for small vehicles, but the supporting high-voltage pulse equipment may lead to scaling problems. Small, high-voltage transformers are available, so perhaps such a system might be applied to a micro air vehicle to improve control. Optimization efforts show several trends in which surface DBDs could be designed to be more effective. If a flow speed of 200-300 m/s can be significantly affected at atmospheric pressure or above, then DBDs could be applied to rotorcraft or turbine blade assemblies.

While DBDs have generally been researched with atmospheric pressure and low speeds, glow discharge phenomena have operated in low pressure, high-speed environments. As was discussed, the effect of glow discharges is generally thermal, which changes the local Mach number and can affect drag and the shock wave structure. Although glow discharges have demonstrated several capabilities during subscale ground tests, some of their trends may be troublesome for high-speed flight. For instance, the glow discharge thermal effect will likely be reduced for higher speeds and higher aerodynamic heating. Short blowdown and shock tube tests may not be able to replicate the steady-state surface heating from a flight. Also, it appears at least some forms of glow discharges are only effective for blunt objects. Furthermore, glow discharges are more difficult to support as pressure is increased. More emphasis should be placed on surface actuators and inlet systems in an effort to advance from low pressure blunt body testing which does not appear to have led to any engineering applications. Although much of the discussion on glow discharges has been skeptical, one area where they make a major impact in aerodynamics is that of plasma-assisted ignition and combustion. Reference 129 provides a thorough experimental review of that field.

Based on recent research, it appears that EMFC actuators have the most promise for high-speed flow control. This can be partially attributed to the fact that more energy can be placed into an EMFC actuator than the other systems. Therefore, power consumption can be high. EMFC systems have one major disadvantage when compared to DBD and glow discharge control: a separate ionization system is needed to generate conductivity for the Lorentz force to take effect for usual aerodynamic conditions. However, new methods of creating non-thermal conductivity by high-frequency pulsed discharges, electron beams, microwaves, radiation, and various combinations are very promising. Increased research into improving the conductivity seen with these systems and operating with higher pressures is recommended.

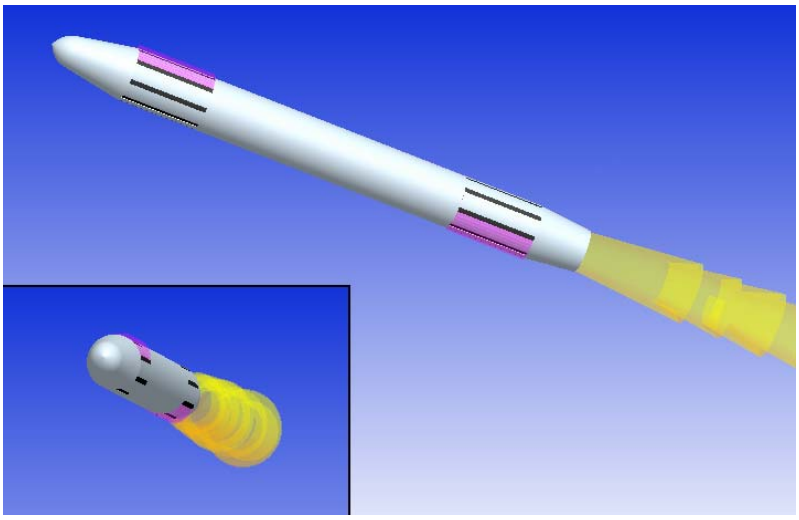

**Figure 25. Example of a future high speed missile with EMFC actuators that could potentially replace conventional control surfaces. Magnets are embedded beneath and between the electrodes (colored black) and diffuse plasma (colored purple) is observed when the controls are actuated.**

Also, proof-of-concept testing of these systems will lead to further understanding of their effectiveness for control surface implementation. Magnet selection is another critical issue. Inexpensive NdFeB magnets can be placed into thin control surfaces, but they may need active cooling in hot aerodynamic environments. It is unknown if the field strength of these magnets will be high enough at this time. Electromagnets and superconducting magnets provide much higher surface fields than NdFeB magnets, but they carry a large weight penalty and must additionally be powered. Although NdFeB magnets have been discussed and tested to some extent in recent publications, more research should be conducted with them contained in compact control surface actuators. Perhaps the best prospects for on-board EMFC with current technology are for improved control of high-speed missiles, which would benefit from surfaces that can actuate rapidly with reduced heating and drag when compared to mechanical actuators. A futuristic depiction is shown in Fig. 25. Power requirements will be raised, but state-of-the-art MEMS microturbine generators may be able to provide the same power input for 5% of the weight of current batteries.[130]

All of these electric and electromagnetic flow control systems are in an early stage of development. Some, if not all, have major design hurdles to overcome before they can be labeled flight-ready technology. However, technical needs coupled with demonstrations of the potential that exists with EMFC and EFC systems make the prospects for further research in this field promising.

## Acknowledgments

The authors would like to thank Dr. J. Craig Dutton of the University of Illinois at Urbana-Champaign for many useful discussions regarding EFC and EMFC as well as Dr. Ramakanth Munipalli of HyPerComp, Inc., for providing a computational MHD program that has been used for the EMFC electric field calculations presented in this paper. The authors are also grateful to Dr. Joseph Shang of Wright State University for providing helpful comments on the manuscript prior to publication. This work was partially supported by the Texas Advanced Research Program, Project No. 003656-0013-2006.

## References

[1]Resler, R. L., and Sears, W. R., "The Prospects for Magneto-Aerodynamics," *Journal of the Aeronautical Sciences*, Vol. 25, No. 4, 1958, pp. 235-245, 258.

[2]Rittenhouse, L. E., Pigott, J. C., Whoric, J. M., and Wilson, D. R., "Theoretical and Experimental Results with a Linear Magnetohydrodynamic Accelerator Operated in the Hall Current Neutralized Mode," AEDC-TR-67-150, Arnold Air Force Station, TN, Nov. 1967.

[3]Rosa, R. J., "Part One: Shock Wave Spectroscopy. Part Two: Engineering Magneto-hydrodynamics," Ph.D. Dissertation, Cornell University, Ithaca, NY, 1956.

[4]Patrick, R. M., "Magneto-hydrodynamics of Compressible Fluids," Ph.D. Dissertation, Cornell University, Ithaca, NY, 1956.

[5]Simmons, G. A., and Nelson, G. L., "Overview of the NASA MARIAH Project and Summary of Technical Results," AIAA Paper 1998-2752, 1998.

[6]Gurijanov, E. P., and Harsha, P. T., "AJAX: New Directions in Hypersonic Technology," AIAA Paper 1996-4609, 1996.

[7]Kuranov, A. L., and Sheikin, E. G., "Magnetohydrodynamic Control on Hypersonic Aircraft Under "Ajax" Concept," *Journal of Spacecraft and Rockets*, Vol. 40, No. 2, 2003, pp. 174-182.

[8]Macheret, S. O., Shneider, M. N., Miles, R. B., and Lipinski, R. J., "Electron-Beam-Generated Plasmas in Hypersonic Magnetohydrodynamic Channels," *AIAA Journal*, Vol. 39, No. 6, 2001, pp. 1127-1138.

[9]Caledonia, G. E., Person, J. C., and Hastings, D., "Ionization Phenomena about the Space Shuttle," AFGL-TR-86-0045, Andover, MA, Jan. 1986.

[10]Holt, A. C., "Electromagnetic Braking for Mars Spacecraft," AIAA Paper 1986-1588, 1986.

[11]Tanifuji, T., Matsuda, A., Wasai, K., Otsu, H., Yamasaki, H., Konigorski, D., and Abe, T., "Expansion Tube Experiment of Applied Magnetic Field Effect on Reentry Plasma," AIAA Paper 2008-1113, 2008.

[12]Palm, P., Meyer, R., Ploenjes, E., Bezant, A., Adamovich, I. V., Rich, J. W., and Gogineni, S., "MHD Effect on a Supersonic Weakly Ionized Flow," AIAA Paper 2002-2246, 2002.

[13]Macheret, S. O., Shneider, M. N., and Miles, R. B., "Modeling of Plasma Generation in Repetitive Ultra-short DC, Microwave, and Laser Pulses," AIAA Paper 2001-2940, 2001.

[14]Shang, J. S., "Recent Research in Magneto-Aerodynamics," *Progress in Aerospace Sciences*, Vol. 37, No. 1, 2001, pp. 1-20.

[15]Bruno, C., Czysz, P. A., and Murthy, S. N. B., "Electro-Magnetic Interactions in a Hypersonic Propulsion System," AIAA Paper 1997-3389, 1997.

[16]Park, C., Mehta, U. B., and Bogdanoff, D. W., "Magnetohydrodynamics Energy Bypass Scramjet Performance with Real Gas Effects," *Journal of Propulsion and Power*, Vol. 17, No. 5, 2001, pp. 1049-1057.

[17]Roth, J. R., "Aerodynamic Flow Acceleration Using Paraelectric and Paristaltic Electrohydrodynamic Effects of a One Atmosphere Uniform Glow Discharge Plasma," *Physics of Plasmas*, Vol. 10, No. 5, 2003, pp. 2117-2126.

[18]Sutton, G. W., and Sherman, A., *Engineering Magnetohydrodynamics*, McGraw-Hill, New York, 1965, Chaps. 2, 8, 10, 12.
[19]Harrington, R. F., *Introduction to Electromagnetic Engineering*, McGraw-Hill, New York, 1958.
[20]Braun, E. M., "Electromagnetic Flow Control: A Review and Development and Testing of a Compact Actuator," Master's Thesis, The University of Texas at Arlington, Arlington, TX, 2008 (to be published).
[21]von Engel, A., *Ionized Gases*, Oxford University Press, London, 1955.
[22]Cobine, J. D., *Gaseous Conductors: Theory and Engineering Applications*, Dover, New York, 1958.
[23]Meyer, R., Nishihara, M., Hicks, A., Chintala, N., Cundy, M., Lempert, W. R., Adamovich, I. V., and Gogineni, S., "Measurements of Flow Conductivity and Density Fluctuations in Supersonic Nonequilibrium Magnetohydrodynamic Flows," *AIAA Journal*, Vol. 43, No. 9, 2005, pp. 1923-1929.
[24]Henoch, C., and Stace, J., "Experimental Investigation of a Salt Water Turbulent Boundary Layer Modified by an Applied Streamwise Magnetohydrodynamic Body Force," *Physics of Fluids*, Vol. 7, No. 6, 1995, pp. 1371-1383.
[25]Macheret, S. O., Shneider, M. N., and Miles, R. B., "Magnetohydrodynamic and Electrohydrodynamic Control of Hypersonic Flows of Weakly Ionized Plasmas," *AIAA Journal*, Vol. 42, No. 7, 2004, pp. 1378-1387.
[26]Gundersen, R. M., "Class of Exact Solutions of Nonisentropic, One-Dimensional Magnetohydrodynamic Flow," *AIAA Journal*, Vol. 1, No. 5, 1963, pp. 1191-1193.
[27]Nishihara, M., Jiang, N., Rich, J. W., Lempert, W. R., Adamovich, I. V., and Gogineni, S., "Low-temperature Supersonic Boundary Layer Control Using Repetitively Pulsed Magnetohydrodynamic Forcing," *Physics of Fluids*, Vol. 17, No. 10, 2005, DOI: 10.1063/1.2084227.
[28]Nishihara, M., Rich, J. W., Lempert, W. R., Adamovich, I. V., and Gogineni, S., "Low-Temperature $M$ = 3 Flow Deceleration by Lorentz Force," *Physics of Fluids*, Vol. 18, No. 8, 2006, DOI: 10.1063/1.2265011.
[29]Palm, P., Meyer, R., Bezant, A., Adamovich, I. V., Rich, J. W., and Gogineni, S., "Feasibility Study of MHD Control of Cold Supersonic Plasma Flows," AIAA Paper 2002-0636, 2002.
[30]Kimmel, R. L., Gogineni, S., Adamovich, I. V., Rich, J. W., and Zhong, X., "Update on MHD Control of Supersonic/Hypersonic Boundary-layer Transition," AIAA Paper 2003-6924, 2003.
[31]Meyer, R., McEldowney, B., Chintala, N., and Adamovich, I. V., "Measurements of Electrical Parameters of a Supersonic Nonequilibrium MHD Channel," AIAA Paper 2003-4279, 2003.
[32]Meyer, R., Chintala, N., Bystricky, B., Hicks, A., Cundy, M., Lempert, W. R., and Adamovich, I. V., "Lorentz Force Effect on a Supersonic Ionized Boundary Layer," AIAA Paper 2004-0510, 2004.
[33]Nishihara, M., Meyer, R., Cundy, M., Lempert, W. R., and Adamovich, I. V., "Development and Operation of a Supersonic Nonequilibrium MHD Channel," AIAA Paper 2004-2441, 2004.
[34]Nishihara, M., Jiang, N., Lempert, W. R., Adamovich, I. V., and Gogineni, S., "MHD Supersonic Boundary Layer Control Using Pulsed Discharge Ionization," AIAA Paper 2005-1341, 2005.
[35]Nishihara, M., Rich, J. W., Lempert, W. R., and Adamovich, I. V., "Low-Temperature M = 3 Flow Deceleration by Lorentz Force," AIAA Paper 2006-1004, 2006.
[36]Nishihara, M., Rich, J. W., Lempert, W. R., and Adamovich, I. V., "MHD Flow Control and Power Generation in Low-temperature Supersonic Flows," AIAA Paper 2006-3076, 2006.
[37]Nishihara, M., Bruzzese, J., Adamovich, I. V., Udagawa, K., and Gaitonde, D., "Experimental and Computational Studies of Low-temperature $M$ = 4 Flow Deceleration by Lorentz Force," AIAA Paper 2007-4595, 2007.
[38]Zaidi, S. H., Smith, T., Macheret, S., and Miles, R. B., "Snowplow Surface Discharge in Magnetic Field for High Speed Boundary Layer Control," AIAA Paper 2006-1006, 2006.
[39]Kalra, C. S., Zaidi, S. H., and Miles, R. B., "Shockwave Induced Turbulent Boundary Layer Separation Control with Plasma Actuators," AIAA Paper 2008-1092, 2008.
[40]Shang, J. S., Kimmel, R., Hayes, J., Tyler, C., and Menart, J., "Hypersonic Experimental Facility for Magnetoaerodynamic Interactions," *Journal of Spacecraft and Rockets*, Vol. 42, No. 5, 2005, pp. 780-789.
[41]Menart, J., Shang, J., Atzbach, C., Magoteaux, S., Slagel, M., and Bilheimer, B., "Total Drag and Lift Measurements in a Mach 5 Flow Affected by a Plasma Discharge and a Magnetic Field," AIAA Paper 2005-947, 2005.
[42]Thibault, J.-P., and Rossi, L., "Electromagnetic Flow Control: Characteristic Numbers and Flow Regimes of a Wall-Normal Actuator," *Journal of Physics D: Applied Physics*, Vol. 36, No. 20, 2003, pp. 2559-2568.
[43]Phillips, O. M., "The Prospects for Magnetohydrodynamic Ship Propulsion," *Journal of Ship Research*, Vol. 6, 1962, pp. 43-51.
[44]Way, S., "Electromagnetic Propulsion for Cargo Submarines," *Journal of Hydronautics*, Vol. 2, No. 2, 1968, pp. 49-57.
[45]Takezawa, S., Tamama, H., Sugawawa, K., Sakai, H., Matsuyama, C., Morita, H., Suzuki, H., and Ueyama, Y., "Operation of the Thruster for Superconducting Electromagnetohydrodynamic Propulsion Ship "Yamato 1"," *Bulletin of the M. E. S. J.*, Vol. 23, No. 1, 1995, pp. 46-55.
[46]Cott, D. W., Daniel, V. W., Carrington, R. A., and Herring, J. S., "MHD Propulsion for Submarines," CDIF External Report No. 2DOE-MHD-D140, Butte, MT, Oct. 1988.
[47]Corke, T. C., and Post, M. L., "Overview of Plasma Flow Control: Concepts, Optimization, and Applications," AIAA Paper 2005-563, 2005.
[48]Roth, J. R., Sin, H., Madhan, R. C. M., and Wilkinson, S. P., "Flow Re-attachment and Acceleration by Paraelectric and Peristaltic Electrohydrodynamic (EHD) Effects," AIAA Paper 2003-531, 2003.

[49]Enloe, C. L., McLaughlin, T. E., VanDyken, R. D., Kachner, K. D., Jumper, E. J., and Corke, T. C., "Mechanisms and Responses of a Single Dielectric Barrier Plasma Actuator: Plasma Morphology," *AIAA Journal*, Vol. 42, No. 3, 2004, pp. 589-594.

[50]Müller, K.-H., Krabbes, G., Fink, J., Gruβ, S., Kirchner, A., Fuchs, G., and Schultz, L., "New Permanent Magnets," *Journal of Magnetism and Magnetic Materials*, Vols. 226-230, Part 2, 2001, pp. 1370-1376.

[51]Magnetic Materials Producers Association, "Standard Specifications for Permanent Magnet Materials," *MMPA Standard No. 0100-00*, 2000.

[52]Brown, R. L., "Benefits and Pitfalls when Using Permanent Magnet Motors in Spinning Applications," *1998 IEEE Annual Textile, Fiber and Film Industry Technical Conference*, Charlotte, North Carolina, 1998.

[53]Liu, J., and Walmer, M., "Designing with High Performance Rare Earth Permanent Magnets," *Proceedings of the 18th International Workshop on High Performance Magnets and Their Applications*, Annecy, France, 2004, pp. 630-636.

[54]Williams, A. J., Walls, R., Davies, B. E., Marchese, J., and Harris, I. R., "A Study of Thermal Demagnetisation Behaviour of Nd-Fe-B Sintered Magnets by a Magnetic Field Mapping System," *Journal of Magnetism and Magnetic Materials*, Vols. 242-245, 2002, pp. 1378-1380.

[55]Hadjipanayis, G. C., Liu, J., Gabay, A., and Marinescu, M., "Current Status of Rare-Earth Permanent Magnet Research in USA," *Journal of Iron and Steel Research, International*, Vol. 13, Suppl. 1, 2006, pp. 12-22.

[56]Liu, J. F., and Walmer, M. H., "Thermal Stability and Performance Data for SmCo 2:17 High-Temperature Magnets on PPM Focusing Structures," *IEEE Transactions on Electronic Devices*, Vol. 52, No. 5, 2005, pp. 899-902.

[57]Liu, J., Vora, P., Dent, P., Walmer, M., Chen, C., Talnagi, J., Wu, S., and Harmer, M., "Thermal Stability and Radiation Resistance of Sm-Co Based Permanent Magnets," *Proceedings of the Space Nuclear Conference 2007*, Paper 2036, Boston, Massachusetts, 2007.

[58]Liu, J., Vora, P., and Walmer, M., "Overview of Recent Progress in Sm-Co Based Magnets," *Journal of Iron and Steel Research, International*, Vol. 13, Suppl. 1, 2006, pp. 319-323.

[59]Braun, E. M., Mitchell, R. R., Nozawa, A., Wilson, D. R., Lu, F. K., and Dutton, J. C., "Electromagnetic Boundary Layer Flow Control Facility Development Using Conductive Particle Seeding," AIAA Paper 2008-1396, 2008.

[60]Shang, J. S., Hayes, J., Harris, S., Umstattd, R., and Ganguly, B., "Experimental Simulation of Magneto-Aerodynamic Hypersonics," AIAA Paper 2000-2258, 2000.

[61]Garrison, G. W., "Electrical Conductivity of a Seeded Nitrogen Plasma," *AIAA Journal*, Vol. 6, No. 7, 1968, pp. 1264-1270.

[62]Jahn, R. G., *Physics of Electric Propulsion*, McGraw-Hill Book Company, New York, 1968.

[63]Stuhlinger, E., *Ion Propulsion for Space Flight*, McGraw-Hill Book Company, New York, 1964.

[64]Oberth, H. J., *Man into Space*, Harper & Row, New York, 1957.

[65]Shepherd, L. R., and Cleaver, A. V., "The Atomic Rocket," *Journal of the British Interplanetary Society*, Vol. 7, 1948, pp. 185; Vol. 8, 1949, pp. 23,50.

[66]Stuhlinger, E., "Electrical Propulsion Systems for Space Ships with Nuclear Power Source," *Journal of Astronautics*, Vol. 2, 1955, pp. 149; Vol. 3, 1956, pp. 11, 33.

[67]Stuhlinger, E., "Flight Path of an Electrically Propelled Space Ship," *Journal of Jet Propulsion*, Vol. 27, No. 4, 1957, pp. 410.

[68]Giannini, G. M., "The Plasma Jet and Its Application," Office of Scientific Research Technical Note 57-520, 1957.

[69]Kantrowitz, A. R., "Introducing Magnetohydrodynamics," *Astronautics*, Vol. 3, No. 10, 1958, pp. 18-20, 74-77.

[70]Frost, L. S., "Conductivity of Seeded Atmospheric Pressure Plasmas," *Journal of Applied Physics*, Vol. 32, No. 10, 1961, pp. 2029-2036.

[71]BenDaniel, D. J., and Bishop, C. M., "Nonequilibrium Ionization in a High-Pressure Cesium-Helium Transient Discharge," *Physics of Fluids*, Vol. 6, No. 2, 1963, pp. 300-306.

[72]Zukoski, E. E., Cool, T. A., and Gibson, E. G., "Experiments Concerning Nonequilibrium Conductivity in a Seeded Plasma," *AIAA Journal*, Vol. 2, No. 8, 1964, pp. 1410-1417.

[73]Cool, T. A., and Zukoski, E. E., "Recombination, Ionization, and Nonequilibrium Electrical Conductivity in Seeded Plasmas," *Physics of Fluids*, Vol. 9, No. 4, 1966, pp. 780-796.

[74]Wolf, R. J., "Electrode Effects in a Seeded Plasma," *AIAA Journal*, Vol. 4, No. 12, 1966, pp. 2155-2159.

[75]Brederlow, G., and Hodgson, R. T., "Electrical Conductivity in Seeded Noble Gas Plasmas in Crossed Electric and Magnetic Fields," *AIAA Journal*, Vol. 6, No. 7, 1968, pp. 1277-1284.

[76]Chu, T. K., and Gottschlich, C. F., "Temperature Measurement of an Alkali Metal-Seeded Plasma in an Electric Field," *AIAA Journal*, Vol. 6, No. 1, 1968, pp. 114-119.

[77]Schweitzer, S., "Tensor Electrical Conductivity of Atmospheric Cesium-Seeded Argon," *AIAA Journal*, Vol. 5, No. 5, 1967, pp. 844-847.

[78]Viegas, J. R., and Kruger, C. H., "Effect of Multispecies Ionization on Electrical Conductivity Calculations," *AIAA Journal*, Vol. 6, No. 6, 1968, pp. 1193-1195.

[79]Polk, D. H., "Measurement of Nonequilibrium Conductivity in Mercury Vapor Seeded with Potassium," *6th Symposium on Engineering Aspects of Magnetohydrodynamics*, AIAA-1965-1032, Pittsburgh, Pennsylvania, 1965.

[80]Rittenhouse, L. E., and Whoric, J. M., "A Physical Model of the Electric Discharge with Cold Electrodes in a Supersonic Seeded Plasma," *6th Symposium on Engineering Aspects of Magnetohydrodynamics*, AIAA-1965-1033, Pittsburgh, Pennsylvania, 1965.

[81]Lu, F. K., Liu, H. C., and Wilson, D. R., "Electrical Conductivity Channel for a Shock Tube," *Measurement Science and Technology*, Vol. 16, No. 9, 2005, pp. 1730-1740.
[82]Hacker, B. C., "Whoever Heard of Nuclear-Powered Ramjets? Project Pluto at Livermore and the Nevada Test Site, 1957-64," *Journal of the International Committee for the History of Technology*, Vol. 1, 1995, pp. 85-98.
[83]Nowak, R., Kranc, S., Porter, R. W., Tuen, M. C., and Cambel, A. B., "Magnetogasdynamic Re-entry Phenomena," *Journal of Spacecraft and Rockets*, Vol. 4, No. 11, 1967, pp. 1538-1542.
[84]Simmons, G. A., Nelson, G. L., and Ossello, C. A., "Electron Attachment in Seeded Air for Hypervelocity MHD Accelerator Propulsion Wind Tunnel Applications," AIAA Paper 1998-3133, 1998.
[85]Elliott, D. G., "Magnetohydrodynamic Power Systems," *Journal of Spacecraft and Rockets*, Vol. 4, No. 7, 1967, pp. 842-846.
[86]Messerle, H. K., *Magnetohydrodynamic Electrical Power Generation*, John Wiley & Sons, New York, 1995.
[87]Mickelsen, W. R., "Auxiliary & Primary Electric Propulsion, Present and Future," *Journal of Spacecraft and Rockets*, Vol. 4, No. 11, 1967, pp. 1409-1423.
[88]Becker, R. A., "Thermionic Space Power Systems Review," *Journal of Spacecraft and Rockets*, Vol. 4, No. 7, 1967, pp. 847-851.
[89]Kalra, C. S., Zaidi, S. H., Alderman, B., Miles, R. B., and Murty, Y. V., "Magnetically Driven Surface Discharges for Shock-Wave Induced Boundary-Layer Separation Control," AIAA Paper 2007-222, 2007.
[90]Kalra, C. S., Zaidi, S. H., Alderman, B., and Miles, R. B., "Non-Thermal Control of Shock-Wave Induced Boundary Layer Separation using Magneto-Hydrodynamics," AIAA Paper 2007-4138, 2007.
[91]Shang, J. S., Hayes, J. R., Miller, J. H., and Menart, J. A., "Magneto-Aerodynamic Interactions in Weakly Ionized Hypersonic Flow," AIAA Paper 2002-349, 2002.
[92]Kimmel, R. L., Hayes, J. R., Menart, J. A., and Shang, J. S., "Effect of Magnetic Fields on Surface Plasma Discharges at Mach 5," AIAA Paper 2004-2661, 2004.
[93]Shang, J. S., Huang, P. G., Yan, H., Surzhikov, S. T., and Gaitonde, D. V., "Hypersonic Flow Control Utilizing Electromagnetic-Aerodynamic Interaction," AIAA Paper 2008-2606, 2008.
[94]Kimmel, R. L., Hayes, J. R., Menart, J. A., and Shang, J. S., "Effect of Magnetic Fields on Surface Plasma Discharges at Mach 5," *Journal of Spacecraft and Rockets*, Vol. 43, No. 6, 2006, pp. 1340-1346.
[95]Menart, J., and Shang, J., "Investigation of Effects Caused by a Pulsed Discharge and a Magnetic Field in a Mach 5 Flow," AIAA Paper 2005-4783, 2005.
[96]Shang, J. S., Kimmel, R., Hayes, J., Tyler, C., and Menart, J., "Hypersonic Experimental Facility for Magnetoaerodynamic Interactions," *Journal of Spacecraft and Rockets*, Vol. 42, No. 5, 2005, pp. 780-789.
[97]Fridman, A., Chirokov, A., and Gutsol, A., "Non-Thermal Atmospheric Pressure Discharges," *Journal of Physics D: Applied Physics*, Vol. 38, No. 2, 2005, pp. R1-R24.
[98]Bletzinger, P., Ganguly, B. N., Van Wie, D., and Garscadden, A., "Plasmas in High Speed Aerodynamics," *Journal of Physics D: Applied Physics*, Vol. 38, No. 4, 2005, pp. R33-R57.
[99]Lowry, H., Stepanek, C., Crosswy, L., Sherrouse, P., Smith, M., Price, L., Ruyten, W., and Felderman, J., "Shock Structure of a Spherical Projectile in Weakly Ionized Air," AIAA Paper 1999-600, 1999.
[100]Ziemer, R. W., "Experimental Investigation in Magneto-aerodynamics," *ARS Journal*, Vol. 19, 1959, pp. 642-647.
[101]Klimov, A. I., Koblov, A. N., Mishin, G. I., Serov, Yu. L., and Yavor, I. P., "Shock Wave Propagation in a Glow Discharge," *Soviet Technical Physics Letters*, Vol. 8, No. 4, 1982, pp. 192-194.
[102]Gorshkov, V. A., Klimov, A. I., Mishin, G. I., Fedotov, A. B., and Yavor, I. P., "Behavior of Electron Density in Weakly Ionized Nonequilibrium Plasma with a Propagating Shock Wave," *Soviet Technical Physics Letters*, Vol. 57, 1987, pp. 1138-1141.
[103]Klimov, A. I., Mishin, G. I., Fedotov, A. B., and Shakhovatov, V. A., "Shock Wave Propagation in a Nonstationary Glow Discharge," *Soviet Technical Physics Letters*, Vol. 15, 1989, pp. 800-802.
[104]Poggie, J., "DC Glow Discharge: A Computational Study for Flow Control Applications," AIAA Paper 2005-5303, 2005.
[105]Shin, J., Narayanaswamy, V., Raja, L. L., and Clemens, N. T., "Characterization of a Direct-Current Glow Discharge Plasma Actuator in Low-Pressure Supersonic Flow," *AIAA Journal*, Vol. 45, No. 7, 2007, pp. 1596-1605.
[106]Menart, J., Henderson, S., Atzbach, C., Shang, J., Kimmel, R., and Hayes, J., "Study of Surface and Volumetric Heating Effects in a Mach 5 Flow," AIAA Paper 2004-2262, 2004.
[107]Merriman, S., Ploenjes, E., Palm, P., and Adamovich, I. V., "Shock Wave Control by Nonequilibrium Plasmas in Cold Supersonic Gas Flows," *AIAA Journal*, Vol. 39, No. 8, 2001, pp. 1547-1552.
[108]Macheret, S. O., Shneider, M. N., and Miles, R. B., "Scramjet Inlet Control by Off-Body Energy Addition: a Virtual Cowl," AIAA Paper 2003-32, 2003.
[109]Shneider, M. N., and Macheret, S. O., "Modeling of Plasma Virtual Shape Control of Ram/Scramjet Inlet and Isolator," *Journal of Propulsion and Power*, Vol. 22, No. 2, 2006, pp. 447-454.
[110]Girgis, I. G., Shneider, M. N., Macheret, S. O., Brown, G. L., and Miles, R. B., "Steering Moments Creation in Supersonic Flow by Off-Axis Plasma Heat Addition," *Journal of Spacecraft and Rockets*, Vol. 43, No. 3, 2006, pp. 607-613.
[111]Mishin, G. I., "Experimental Investigation of the Flight of a Sphere in Weakly Ionized Air," AIAA Paper 1997-2298, 1997.

[112]Ganiev, Y. C., Gordeev, V. P., Krasilnikov, A. V., Lagutin, V. I., Otmennikov, V. N., and Panasenko, A. V., "Aerodynamic Drag Reduction by Plasma and Hot-Gas Injection," *Journal of Thermophysics and Heat Transfer*, Vol. 14, No. 1, 2000, pp. 10-17.
[113]Suchomel, C. F., Van Wie, D., and Risha, D., "Perspectives on Cataloging Plasma Technologies Applied to Aeronautical Sciences," AIAA Paper 2003-3852, 2003.
[114]Fomin, V. M., Maslov, A. A., Malmuth, N. D., Fomichev, V. P., Shashkin, A. P., Korotaeva, T. A., Shiplyuk, A. N., and Pozdnyakov, G. A., "Influence of a Counterflow Plasma Jet on Supersonic Blunt-Body Pressures," *AIAA Journal*, Vol. 40, No. 6, 2002, pp. 1170-1177.
[115]Kogelschatz, U., Eliasson, B., and Egli, W., "From Ozone Generators to Flat Television Screens: History and Future Potential of Dielectric-Barrier Discharges," *Pure and Applied Chemistry*, Vol. 71, No. 10, 1999, pp. 1819-1828.
[116]Okazaki, S., Kogoma, M., Uehara, M., and Kimura, Y., "Appearance of Stable Glow Discharge in Air, Argon, Oxygen, and Nitrogen at Atmospheric Pressure Using a 50 Hz Source," *Journal of Physics D: Applied Physics*, Vol. 26, No. 5, 1993, pp. 889-892.
[117]Roth, J. R., Sherman, D. M., and Wilkinson, S. P., "Boundary Layer Flow Control with a One Atmosphere Uniform Glow Discharge Surface Plasma," AIAA Paper 1998-328, 1998.
[118]Massines, F., Rabehi, A., Decomps, P., Ben Gadri, R., Ségur, P., and Mayoux, C., "Experimental and Theoretical Study of a Glow Discharge at Atmospheric Pressure Controlled by Dielectric Barrier," *Journal of Applied Physics*, Vol. 83, No. 6, 1998, pp. 2950-2957.
[119]Moreau, E., "Airflow Control by Non-Thermal Plasma Actuators," *Journal of Physics D: Applied Physics*, Vol. 40, No. 3, 2007, pp. 605-636.
[120]Corke, T. C., Post, M. L., and Orlov, D. M., "SDBD Plasma Enhanced Aerodynamics: Concepts, Optimization and Applications," *Progress in Aerospace Sciences*, Vol. 43, No. 7, 2007, pp. 193-217.
[121]Jayaraman, B., and Shyy, W., "Modeling of Dielectric Barrier Discharge-Induced Fluid Dynamics and Heat Transfer," *Progress in Aerospace Sciences*, Vol. 44, No. 3, 2008, pp. 139-191.
[122]Roth, J. R., Madhan, R. C. M., Yadav, M., Rahel, J., and Wilkinson, S. P., "Flow Field Measurements of Paraelectric, Parastaltic, and Combined Plasma Actuators Based on the One Atmosphere Uniform Glow Discharge Plasma (OAUGDP$^{TM}$)," AIAA Paper 2004-845, 2004.
[123]Roth, J. R., and Dai, X., "Optimization of the Aerodynamic Plasma Actuator as an Electrohydrodynamic (EHD) Electrical Device," AIAA Paper 2006-1203, 2006.
[124]Enloe, C. L., McLaughlin, T. E., VanDyken, R. D., Kachner, K. D., Jumper, E. J., Corke, T. C., Post, M., and Haddad, O., "Mechanisms and Responses of a Single Dielectric Barrier Plasma Actuator: Geometric Effects," *AIAA Journal*, Vol. 42, No. 3, 2004, pp. 595-604.
[125]Opaits, D. F., Roupassov, D. V., Starikovskaia, S. M., Starikovskii, A. Yu., Zavialov, I. N., and Saddoughi, S. G., "Plasma Control of Boundary Layer Using Low-Temperature Non-Equilibrium Plasma of Gas Discharge," AIAA Paper 2005-1180, 2005.
[126]Roupassov, D. V., Zavyalov, I. N., and Starikovskii, A. Yu., "Boundary Layer Separation Plasma Control Using Low-Temperature Non-Equilibrium Plasma of Gas Discharge," AIAA Paper 2006-373, 2006.
[127]Sidorenko, A. A., Budovsky, A. D., Pushkarev, A. V., and Maslov, A. A., "Flight Testing of a DBD Plasma Separation Control System," AIAA Paper 2008-373, 2008.
[128]Enloe, C. L., McLaughlin, T. E., VanDyken, R. D., Kachner, K. D., Jumper, E. J., and Corke, T. C., "Mechanisms and Responses of a Single Dielectric Barrier Plasma," AIAA Paper 2003-1021, 2003.
[129]Starikovskaia, S. M., "Plasma Assisted Ignition and Combustion," *Journal of Physics D: Applied Physics*, Vol. 39, No. 16, 2006, pp. R265-R299.
[130]Fleeman, E. L., *Tactical Missile Design*, 2nd ed., AIAA Education Series, AIAA, Reston, VA, 2006, Chap. 8.